

AD-769 972

SPUTTERED THIN FILM RESEARCH

Alexander J. Shuskus, et al

United Aircraft Research Laboratories

Prepared for:

Office of Naval Research

October 1973

DISTRIBUTED BY:

NTIS

**National Technical Information Service
U. S. DEPARTMENT OF COMMERCE
5285 Port Royal Road, Springfield Va. 22151**

Unclassified

Security Classification

AD-769 972

DOCUMENT CONTROL DATA - R & D

(Security classification of title, body of abstract and indexing annotation must be entered when the overall report is classified)

1. ORIGINATING ACTIVITY (Corporate author) United Aircraft Corporation Research Laboratories East Hartford, Connecticut 06108		2a. REPORT SECURITY CLASSIFICATION Unclassified	
3. REPORT TITLE Sputtered Thin Film Research		2b. GROUP	
4. DESCRIPTIVE NOTES (Type of report and inclusive dates) Semi-Annual Report for the Period 16 April 1973 to 30 September 1973			
5. AUTHOR(S) (First name, middle initial, last name) A. J. Shuskus, D. J. Quinn, E. L. Paradis, J. M. Berak and D. E. Cullen			
6. REPORT DATE October 1973		7a. TOTAL NO. OF PAGES 59	7b. NO. OF REFS
8a. CONTRACT OR GRANT NO. N00014-72-C-0415		8b. ORIGINATOR'S REPORT NUMBER(S) M951337-9	
b. PROJECT NO. c. ARPA Order No. 2173, Amendment No. 1		9b. OTHER REPORT NO(S) (Any other numbers that may be assigned this report)	
10. DISTRIBUTION STATEMENT			
11. SUPPLEMENTARY NOTES Details of illustrations in this document may be better studied on microfiche.		12. SPONSORING MILITARY ACTIVITY Department of the Navy Office of Naval Research	
13. ABSTRACT Progress on the process development as it relates to the optical quality of sputtered single crystal films of ZnO, AlN, and TiO ₂ is discussed. Optical attenuation data for optical waveguide structures comprised of zinc oxide, aluminum nitride, titanium dioxide films grown on sapphire substrates and titanium dioxide on YZ cut lithium niobate is presented. The effect of deposition parameters on the carrier mobility of single crystal gallium arsenide films grown by reactive sputtering is presented.			

Reproduced by
NATIONAL TECHNICAL
INFORMATION SERVICE
U S Department of Commerce
Springfield VA 22151

DD FORM 1473
1 NOV 55

Unclassified

Security Classification

14. KEY WORDS	LINK A		LINK B		LINK C	
	ROLE	WT	ROLE	WT	ROLE	WT
Thin Films Reactive Sputtering Single Crystal Aluminum Nitride Zinc Oxide Rutile Gallium Arsenide Optical Waveguiding Epitaxy						

ia

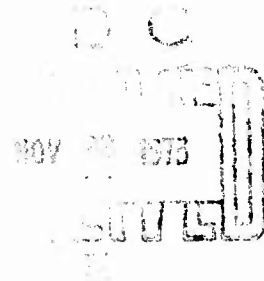
UNITED AIRCRAFT CORPORATION
RESEARCH LABORATORIES
East Hartford, Connecticut

M951337-9

Third Semi-Annual Report Under Contract N00014-72-C-0415
16 April 1973 to 30 September 1973

ARPA Order No.:	2173, Amendment No. 1
Program Cost Code:	000003D10K21
Contractor:	United Aircraft Research Laboratories
Effective Date of Contract:	15 April 1972
Contract Expiration Date:	30 September 1973
Amount of Contract:	\$273,707.00
Contract Number:	N00014-72-C-0415
Contract Management:	Dr. Anthony J. DeMaria (203) 565-3545
Principal Investigator:	Dr. Alexander J. Shuskus (203) 565-6498
Scientific Officer:	Dr. Van Nicolai
Short Title:	Sputtered Thin Film Optics
Reported By:	A. J. Shuskus, D. J. Quinn, E. L. Paradis, J. M. Berak and D. E. Cullen.

Sponsored by Advanced Research Projects Agency
ARPA Order No. 2173, Amendment No. 1



The views and conclusions contained in this document are those of the authors and should not be interpreted as necessarily representing the official policies, either expressed or implied, of the Advanced Research Projects Agency or the U. S. Government. Reproduction in whole or in part is permitted for any purpose of the United States Government.

Report M951337-9

Interim Technical Report Under Contract N00014-72-C-0415
for the Period 16 April 1973 through 30 September 1973

Sputtered Thin Film Research

ARPA Order No. 2173, Amendment No. 1, Project Code 3D10

TABLE OF CONTENTS

	<u>Page</u>
LIST OF ILLUSTRATIONS	iii
LIST OF TABLES	v
1.0 TECHNICAL REPORT SUMMARY	1-1
1.1 Program Objective	1-1
1.2 Major Accomplishments	1-1
1.3 Future Work	1-2
2.0 OPTICAL WAVEGUIDING AND OPTIMIZATION OF DEPOSITION PARAMETERS	2-1
2.1 Apparatus for Optical Waveguide Evaluation	2-1
2.2 Computational Aids to Thin Film Waveguide Studies	2-3
2.3 Optical Waveguide Measurements on Ta ₂ O ₅ , ZnO, AlN and TiO ₂ Films	2-3
2.4 Optimization of Film Deposition Parameters	2-6
2.5 Future Work	2-8
3.0 GROWTH OF EPITAXIAL GALLIUM ARSENIDE FILMS	3-1
3.1 Sputter Ion Spectroscopy of a GaAs Film	3-1

TABLE OF CONTENTS
(cont'd)

	<u>Page</u>
3.2 Electron Microprobe Determination of GaAs Stoichiometry	3-2
3.3 Effect of Deposition Parameters on Sputtered GaAs	3-3
3.4 Optical Considerations and Results	3-5
3.5 Sputtered Indium Antimonide Films	3-6
3.6 Conclusions	3-7
3.7 Future Work	3-8
4.0 GROWTH OF SPUTTERED LASER MATERIALS	4-1
5.0 REFERENCES	5-1

LIST OF ILLUSTRATIONS

- Figure 2.1 Apparatus for Studying Waveguiding in Thin Films
- Figure 2.2 Sample Table and Attenuation Measuring Apparatus
- Figure 2.3 Experimental Setup for Optical Attenuation Measurements
- Figure 2.4 Ta_2O_5 Film on 7059 Glass Waveguiding
- Figure 2.5 Ta_2O_5 Film on 0.1 μ Finish Sapphire Substrate
- Figure 2.6 Single Crystal ZnO Waveguiding
- Figure 2.7 Sample No. ZnO-37, ZnO on Al_2O_3 ($1\bar{1}02$)
- Figure 2.8 Sample No. 119, AlN on Al_2O_3 (0001)
- Figure 2.9 Sample No. 36, TiO_2 on $LiNbO_3$
- Figure 2.10 Electron Micrograph of TiO_2 on (0001) Al_2O_3 No Axial Field RF Power 150W
- Figure 2.11 Electron Micrograph of TiO_2 on ($1\bar{1}02$) Al_2O_3 No Axial Field RF Power 150W
- Figure 2.12 Electron Micrograph of TiO_2 on (0001) Al_2O_3 No Axial Field RF Power 300W
- Figure 2.13 Electron Micrograph of TiO_2 on (0001) Al_2O_3 Axial Field RF Power 300W
- Figure 2.14 Electron Micrograph of TiO_2 on ($1\bar{1}02$) Al_2O_3 Axial Field RF Power 300W
- Figure 3.1 Sputter-Ion Mass Spectrum of a GaAs Film
- Figure 3.2 Minimum Film Thickness Required to Support $m = 0$ Mode Vs. Index Difference Between Film and Substrate
- Figure 3.3 RED of (111) InSb - Beam Along $[\bar{2}11]$
- Figure 3.4 RED of (111) InSb - Beam Along $[1\bar{1}0]$

M951337-9

Figure 3.5 RED of InSb on (100) GaAs - Beam Along [100]

Figure 3.6 RED of InSb on (100) GaAs - Beam Along [100]

LIST OF TABLES

Table 2-I	Sample ZnO-37
Table 3-I	Mass Spectrograph Analysis of a Gallium Arsenide Film (Sample Ga-23)
Table 3-II	Determination of Stoichiometry by Electron Microprobe Analysis
Table 3-III	Deposition Conditions and Electrical Properties of GaAs Films
Table 3-IV	Deposition Parameters for InSb Films
Table 3-V	Electrical Properties of InSb Films
Table 4-I	Powder X-Ray Diffraction Data for $\text{NdP}_{514}\text{O}_{14}$

1.0 SUMMARY

1.1 Program Objective

The major objective of the program is to establish the feasibility of reactive rf sputtering for the preparation of single crystal thin films suitable for applications in microelectronics, microwave devices and integrated optics. Materials of interest include selected III-V and II-VI semiconductors and high dielectric constant materials. A secondary objective of the program is the fabrication of devices to ascertain the device potential of the material prepared by sputtering. This program is being conducted under the ARPA/ONR Contract N00014-72-C-0415.

1.2 Major Accomplishments

Over the course of the last six months significant progress has been made in improving the optical quality of the single crystal films grown by sputtering. Results for optical waveguiding for the combinations of aluminum nitride on sapphire, titanium dioxide on sapphire and titanium dioxide on YZ cut lithium niobate are reported for the first time.

Facilities have been setup for the study of optical waveguiding in thin films. Lasers covering the range of the spectrum from 0.6328 μm to 3.39 μm are employed to characterize waveguiding qualities of the films grown. Provisions have been made for accurate attenuation measurements. Two computer programs have been written to aid in the evaluation of the waveguide films and to serve as a guide in processing of the films.

Through modifications of the sputtering systems and deposition parameter studies marked improvement in the optical qualities of films grown by sputtering has been achieved. Zinc oxide films grown on (1102) sapphire substrates initially exhibited optical waveguiding losses of 40 dB/cm at a wavelength of 0.6328 μm and this has been reduced to 18 dB/cm. At 1.06 μm the losses are 6.5 dB/cm. The measured optical loss for AlN and TiO₂ films initially was in the range of 100 dB/cm. For aluminum nitride grown on (0001) sapphire substrates the losses have been reduced to 30 dB/cm at 0.6328 μm and 16 dB/cm at 1.06 μm . Rutile films on (1102) sapphire substrates have shown losses as low as 20 dB/cm at 0.6328. Titanium dioxide films grown on YZ cut lithium niobate substrates have exhibited optical losses of 28 dB/cm at 0.6328 μm . The optical waveguiding results quoted for aluminum nitride and titanium dioxide, are to our knowledge, the first results of their kind for these materials.

The fixtures required for the reactive sputtering of gallium nitride have been fabricated and assembled. Studies on epitaxial deposition of gallium nitride on sapphire and spinel have been initiated.

Neodymium ultraphosphate was synthesized and sufficient material was produced to fabricate a four inch diameter sputtering target.

The work on gallium arsenide has been mainly concerned with determining the cause of the low carrier mobility in single crystal films grown by reactive sputtering. Experimental evidence has shown that the low mobility results from the presence of structural defects. The deposition parameters have been shown to affect the Hall mobility, and these trends are being pursued in an effort to optimize the sputtering conditions. Preliminary experiments to determine the optical waveguide properties of the sputtered films have been initiated.

1.3 Future Work

Although significant progress has been made in the reduction of optical loss in single crystal films of ZnO, AlN and TiO₂ grown by reactive sputtering, additional work is required. Efforts will continue with deposition parameter studies. Structural quality of the films will continue to be evaluated by x-ray and electron diffraction. Films will be sectioned and examined by electron microscopy for gross structural defects which may affect the optical properties. Growth and evaluation of single crystal films of gallium nitride will be pursued. Studies to improve the carrier mobility of the gallium arsenide grown by sputtering will continue. The study of the properties of sputtered neodymium ultraphosphate films will be initiated. The feasibility of this material as a thin film laser and amplifier will be evaluated. Thin film devices employing either acoustooptic or electrooptic interactions will be fabricated to further evaluate the potential of sputtered ZnO, TiO₂, AlN and GaAs single crystal films for integrated optics applications.

2.0 OPTICAL WAVEGUIDING AND OPTIMIZATION OF FILM DEPOSITION PARAMETERS

Facilities have been setup for the study of optical waveguiding in thin films. Lasers covering the range of the spectrum from 0.633 μm (red) to 3.39 μm (infrared) are employed to characterize the waveguiding qualities of the films grown. Provisions have been made for obtaining accurate attenuation measurements. Numerous films of ZnO, ALN, and TiO₂, grown by reactive sputtering have been examined for waveguiding. The best results to date are for ZnO on (1102) Al₂O₃; however, films of ALN and TiO₂ on Al₂O₃ and films of TiO₂ on LiNbO₃ also exhibit waveguiding with losses as low as 16 dB/cm at 1.059 μm . Both prism and grating coupling techniques have been investigated. A series of amorphous Ta₂O₅ films were grown on glass substrates to provide samples with which to learn the experimental techniques of coupling to a thin film waveguide. The ability to produce waveguide quality Ta₂O₅ films has proven useful in other aspects of this study including the rapid evaluation of substrate materials by examination of the ability of a Ta₂O₅ film grown on such a substrate to support guided modes. In addition to the experimental studies, two computer programs have been written to aid in the evaluation of the waveguide films and to serve as a guide in the processing of the films.

2.1 Apparatus for Optical Waveguide Evaluation

A photograph of the apparatus used for studying waveguiding in thin films is shown in Fig. 2.1. Three lasers are regularly employed. A small 0.5 mW, 0.633 μm , He-Ne laser is used for alignment purposes and for rough evaluation of newly made films. The larger He-Ne laser, with a stable output of 15 mW at 0.633 μm , is used for most attenuation measurements. This unit has also been converted for use at 1.150 μm and 3.391 μm whenever the need has arisen. A homemade Nd:YAG laser with an output of over 100 mW at 1.059 μm provides ample light for visual observation of the films using a small battery powered Varo infrared to visible converter. The ability to actually observe the guided wave via the converter greatly simplifies the procedure of examining the films for waveguiding. In addition to the three lasers shown in Fig. 2.1, other lasers with outputs in the blue and green regions of the spectrum and at 10.6 μm are available on a loan basis when required.

The sample table and attenuation measuring apparatus is shown in greater detail in Fig. 2.2. A waveguide film on a small substrate is shown mounted in the prism-film coupling jig on top of the turntable. Provisions have been made for properly orienting the plane of the film with respect to the laser beam. Light from one of the lasers is focused onto the coupling prism by a simple lens. The beam also passes through a polarizer and a 0.5° wedge that can be rotated about a horizontal axis and thus used to scan the prism-film contact region in a vertical direction. Angular resolution of the turntable is $\sim 0.01^\circ$ making possible accurate determination of the angles at which light is coupled into the film.

Light can be coupled into thin films using prisms or gratings, or the laser beam can be focused onto a cleaved or tapered edge of the film to obtain guiding. Prisms and gratings have the advantage that any desired mode of light-wave propagation can be efficiently and selectively excited, and the difficult problem of focusing the beam onto the film edge is avoided. Attempts have been made to edge couple 1.059 μm light into a sputtered GaAs film; however, waveguide modes were not detected. The prism-film coupler has been more widely used in the present study. The small jig shown in Fig. 2.2 is used to apply pressure between the coupling prism and the thin film. A small round rod beneath the substrate, located ~ 1 mm back of the right angle corner of the prism (see Fig. 2.3), is used to localize the pressure between prism and film and thus reduce the air gap between prism and film to a thickness small enough ($\lesssim \lambda/4$) for efficient coupling (Refs. 1,2). This restriction on the size of the gap can be relaxed somewhat by using an index matching fluid. For a given gap spacing, the addition of an index matching fluid will increase the coupling efficiency and these fluids have been used for just that purpose. The prisms used in this effort are 35° rutile prisms cut with the C-axis parallel to the right angle edge of the prism. With these prisms, waveguide modes with propagation constants (β/k) values as high as 2.17 for TM modes and 2.34 for TE modes can be accessed.

The facilities for fabricating photoresist grating couplers by an optical interference techniques (Ref. 3) are available and gratings have been produced with a periodicity of 0.7 μm with no difficulty. Such gratings have not, as yet, been put on waveguide films, primarily because of the simplicity and convenience of the prism-film coupling technique. Gratings are necessary, however, for coupling to GaAs films and hence when the proper laser becomes available, the setup for fabricating gratings will be assembled again.

Attenuation measurements have been made in two ways. Originally, these measurements were made using a fiber optic technique similar to that described by Goell and Standley (Ref. 4). One end of an 0.5 mm dia. optical fiber is mounted on an x-y-z micro-positioner such that it can be positioned close (< 1 mm separation) to the surface of the waveguide film and traversed in the plane of the film. The other end of the fiber is rigged so that the light output falls on the cathode of the photo-multiplier of a Pritchard photometer. The fiber optic probe is then used to measure the intensity of the light scattered from the guided beam as a function of distance along the beam. From this data the attenuation of the film, in dB/cm, can readily be obtained. This method works well when large substrates are used. Many of the films in this study are grown on rather small substrates to conserve expensive substrate material and, under these conditions, the fiber optic probe technique is unsatisfactory.

An alternative method of measuring the light scattered from the guided mode uses a simple lens to form an image of the light streak in the film and a narrow slit in front of a photodetector is then scanned along the image (Ref. 1). The

experimental setup of this method is shown in Fig. 2.2 and is illustrated schematically in Fig. 2.3. A mechanical chopper modulates the laser beam and a phase sensitive amplifier is used to recover the low level signal from the photodetector. Corrections for image size are not necessary if a true size image is generated.

It is assumed, in using either of the two methods outlined above, that the scattering centers are uniformly distributed in the film. Both methods work well for losses as low as 1 dB/cm. Below 1 dB/cm, the variability in the location and strength of the scattering centers makes reliable measurements difficult. Measurements made on several Ta_2O_5 films using both methods show good agreement. Losses for these films are typically 3 dB/cm with some Ta_2O_5 films showing losses as low as 1 dB/cm as reported by Tien (Ref. 1).

2.2 Computational Aids to Thin Film Waveguide Studies

A knowledge of the angle and polarization of the incident laser beam for which guided modes are obtained in a given film enables one to compute the refractive index (N_F) and thickness (W) of that film. A computer program has been written to perform this calculation. Using an estimated index as a starting point, the computer calculates a film thickness for each mode observed. The mean thickness and deviation are then calculated, and the computer then iterates on the index until the thickness deviation is minimized. This method provides an accurate way of determining both N_F and W of a thin film waveguide. Accuracies of 1% for N_F have been obtained (Ref. 4).

In cases where the film will support only one waveguide mode, or only one mode can be coupled into the film because of prism or grating limitations, N_F and W can still be determined with the aid of another computer program written for this study. This second program computes the allowed modes for a film of given N_F and W . The $N_F \cdot W$ product of the film is first determined from measurements of the transmitted or reflected intensity versus wavelength. A series of computations are then made using values of N_F and W that give the correct $N_F \cdot W$ product. The propagation constant, β/k , is then plotted versus N_F and the value of β/k for the observed mode is used to pinpoint the true N_F and hence W as well. This method has been used for many of the TiO_2 films since they usually are only $\sim 0.5 \mu m$ thick and their high index means that often the low order modes cannot be accessed with the present 35° rutile prisms.

2.3 Optical Waveguide Measurements on Ta_2O_5 , ZnO, AlN and TiO_2 Films

Waveguide films of amorphous Ta_2O_5 have been grown on Corning 7059 glass substrates by reactive sputtering. Early attempts to fabricate waveguide films by oxidizing sputtered Ta films proved to be unsuccessful. While the oxidized films appear clear and cannot be distinguished from the reactively sputtered Ta_2O_5 films

either by eye or with an optical microscope, they will not support guided modes. The reasons for this are not apparent, but it is conjectured that the oxidized films may contain microcracks resulting from stresses built up during either the deposition of the Ta or the subsequent oxidation.

The reactively sputtered Ta_2O_5 films are typically 2 μm thick and support approximately 20 guided modes, all of which propagate the length of the 3 inch glass substrate (see Fig. 2.4). These films are grown in a 10 μ torr argon ambient containing 40% oxygen with an rf power of 200 watts applied to the 4 inch diameter Ta target.

In addition to their usefulness during the initial stages of the program when the experimental details of the prism-film coupling technique were being learned, the Ta_2O_5 films have been utilized more recently to assess the surface finish of substrate materials. Sapphire substrates from two suppliers, A. Meller, Co. and INSACO, Inc., have been used in the sputtered thin film research. Single crystal films of ZnO, AlN, and TiO_2 have been grown on substrates from both suppliers; however, waveguiding was not observed in many cases. The surface finish on the original batches of substrates from both Meller and INSACO was labeled as having an epitaxial grade finish. To determine whether substrate finish was instrumental in preventing waveguiding, Ta_2O_5 films were simultaneously sputtered on samples of sapphire from the different suppliers along with a piece of 7059 glass. The Ta_2O_5 films on the 7059 glass and on the 0.1 μ inch sapphire substrate from INSACO, Inc. exhibited waveguiding while the other did not. Figure 2.5a shows a film mode propagating in a Ta_2O_5 film on the INSACO substrate. (The milky appearance of the film-substrate sandwich is due to the fact that the back side of the substrate was not polished.) Under the same conditions, no film mode was observed in the Ta_2O_5 film on the Meller substrate. Rather, a continuum of substrate modes emanated from the corner of the prism (Fig. 2.5b) indicating that the light coupled into the film at the particular synchronous angle was quickly scattered by the surface roughness of the substrate into substrate modes. Only 0.1 μ inch finish INSACO substrates are now being used.

Optical waveguiding has been achieved in as-sputtered ZnO films on (1102) sapphire substrates. X-ray diffraction and reflection electron diffraction studies of these ZnO films have shown them to be single crystal with a (1120) orientation. This is the preferred orientation for best electrooptic and acoustooptic interactions. The as-deposited films have resistivities $\geq 10^6 \Omega\text{-cm}$. They therefore do not require compensation by lithium or sodium diffusion to increase their resistivity to a usable value. Electron micrographs of replicated surfaces show the surface quality of the sputtered ZnO films to be excellent and requires no mechanical polishing prior to use.

Figure 2.6 is a photograph of the first ZnO film to exhibit waveguiding. The photo shows the film mounted in the prism coupler jig with the incoming 0.633 μm laser beam and the guided wave in the film clearly visible. The losses in this

sample were measured to be in the 45-50 dB/cm range. More recent films exhibit significantly lower losses. Figure 2.7 is a plot of the intensity of scattered light versus distance along the light streak for a TE $M = 0$ mode in a recent ZnO film. Losses calculated from the slope of the lines is 18 dB/cm at 0.633 μm and 6.5 dB/cm at 1.059 μm . This film supported 4 TE and 4 TM modes. The increase in the loss with increasing mode is in accordance with the elementary surface scattering theory presented by Tien (Ref. 1).

The index and thickness of this film were calculated using the computer program mentioned earlier. A knowledge of θ (see Fig. 2.3) for which waveguiding was obtained and the indices and angle of the rutile prism allows one to obtain the pre-propagation constant, β/k , for each mode. The computer then treats N_F and W as free parameters and adjusts them for a best fit to the observed β/k 's. The thickness thus determined was $1.372 \pm .010 \mu\text{m}$ and the index was 2.002 for TE modes and 1.991 for TM modes. Using these values of N_F and W , theoretical values of β/k for both TE and TM modes were then calculated and the results are presented in Table 2-I along with the observed β/k 's. The direction of propagation of the guided modes was perpendicular to the C-axis of the film; hence, the TE modes propagate as extraordinary rays in the ZnO film. The value of $N_F = 2.002$ determined for this sample is very close to the value of 2.003 interpolated from measurements on bulk ZnO by Bond (Ref. 5). This agreement supports the x-ray, RED, and resistivity data in indicating excellent crystalline perfection of our sputtered ZnO films.

While the optical losses in our ZnO films are higher than those recently reported by Hammer, et al (Ref. 6), for ZnO films grown by CVD, several important points should be noted. First, the low attenuation of the CVD films was obtained only after polishing. Losses were not quoted for the as-deposited films. Second, the CVD films were typically 10 μm thick, whereas our results are for relatively thin $\sim 1 \mu\text{m}$ films where surface scattering losses are an order of magnitude higher than they would be for a 10 μm film. A third point is that the CVD films are low resistivity films and therefore require compensation by diffusion. CVD ZnO films with the desirable (11 $\bar{2}$ 0) orientation grown recently by Brady, et al, IBM (Ref. 7) showed "poor optical quality" and no attenuation values were quoted.

Figure 2.8 is a plot of scattered light intensity versus distance along the guided beam for AlN sample No. 119. The attenuation values of 33 dB/cm at 0.633 μm and 16 dB/cm at 1.059 μm are the best obtained to date for AlN on sapphire. These films are not polished, but are examined in the as-sputtered condition. Losses for AlN on (11 $\bar{2}$ 0) sapphire are higher. The index of refraction for the AlN films has been determined to be 2.15. To our knowledge the optical waveguide data quoted above for aluminum nitride films on sapphire is the first published data for this material.

Waveguiding has been obtained for as-sputtered TiO₂ films on both Al₂O₃ and LiNbO₃. Losses are typically $\lesssim 30$ dB/cm at 0.633 μm for either substrate material

(see Fig. 2.9). Most of these films have been rather thin, $\sim 0.5 \mu\text{m}$ or less, so that $1.059 \mu\text{m}$ modes either are not allowed or the limitations of the 35° rutile prisms prohibits coupling to the allowed modes. As a result, attenuation data for TiO_2 films at $1.059 \mu\text{m}$ is not available at this time. A new set of 45° rutile prisms are to be ordered for use with these higher index films. Values of N_F determined from a combination of transmission measurements and waveguiding measurements are 2.55 for TiO_2 on LiNbO_3 and 2.18 for TiO_2 on Al_2O_3 . Thicker films are being prepared for evaluation at $1.06 \mu\text{m}$ wavelength. The optical waveguiding data presented here is the first reported in the literature for single crystal titanium dioxide films.

2.4 Optimization of Film Deposition Parameters

In the previous semi-annual report successful epitaxial growth of aluminum nitride, zinc oxide, titanium dioxide and gallium arsenide was reported. During this report period efforts were directed toward evaluating the optical properties of the films grown. Initial optical waveguiding experiments showed that the optical losses were relatively high and that adjustments were required in the deposition parameters to improve matters. Modifications in the sputtering chamber were also required due to problems arising from fallout of particulate matter onto the substrate as a result of flaking from fixtures and shutters. This was particularly troublesome with the aluminum nitride and titanium dioxide systems because of the radiant heating due to the substrate heater operation at 1000°C or greater. These problems were overcome to a large extent by changing the design of the shutters used in sputter cleaning and modifying to the fixtures in the sputtering chamber.

Aluminum Nitride

In our initial studies, deposition parameters such as substrate temperature, ambient pressure, cooling rate, etc. had little effect on improving the optical quality of the aluminum nitride films. Subsequently it was found that the parameter which provided the most significant improvement in the optical quality of the films was an increase in the deposition rate. We were able to increase the deposition rate from $50 \text{ \AA}/\text{min}$ to $100 \text{ \AA}/\text{min}$ for (0001) oriented ALN and still maintain single crystal growth. Optical loss was dramatically reduced from $100 \text{ dB}/\text{cm}$ to $\sim 30 \text{ dB}/\text{cm}$ at a wavelength of 6328 \AA . The effects of the previously mentioned parameters will have to be re-examined because with initial losses so high small improvements gained would tend to be masked.

The maximum deposition rate for single crystal growth of (0001) oriented ALN films has not been established since the rf power that can be coupled into the system has been limited by the power handling capability of the matching network. This matching network is being reworked in order to remove this constraint on rf power

level and hence deposition rate. Efforts will continue to establish the maximum deposition rate for growth of (0001) oriented aluminum nitride films and its ultimate effect on optical loss.

It was found that a deposition rate in excess of 50 Å/min would result in polycrystalline deposits of AlN on (1102) oriented sapphire substrate. The reason for the high optical loss observed in (1120) aluminum nitride films remains to be determined. Further studies on the variation of deposition parameters will be required to further improve the optical quality of the sputtered films. Films of aluminum nitride have also been grown on (110) and (111) oriented spinel substrates and are currently undergoing evaluation. The fairly significant improvement achieved in optical quality of the AlN films during this report period lend encouragement that even lower loss films of aluminum nitride can be prepared.

Titanium Dioxide

The surface texture of rutile films first grown on (0001) and (1102) sapphire has been relatively rough and has resulted in excessive surface scattering losses in the course of optical waveguide studies. The films grown generally were thin and did not readily lend themselves to polishing. Figures 2.10 and 2.11 show electron micrographs of replicated surfaces of some of the early rutile films grown on (0001) and (1102) sapphire substrates. In the course of the deposition parameter studies, an increase in the deposition rate was found to be the most significant parameter in reducing optical loss as was the case for aluminum nitride. The improved surface finish resulting from an increased deposition rate is illustrated in Fig. 2.12. Further improvement in the surface finish was gained by the application of an axial magnetic field of 50 gauss at the substrate. The resulting improvement is shown in Figs. 2.13 and 2.14. Deposition rates have been increased from 20 Å/min to 50 Å/min. The matching network for the TiO₂ system has been rebuilt to accommodate higher rf power levels and the effects of even higher deposition rates are under evaluation.

Titanium dioxide films have also been grown on YZ cut lithium niobate substrates. At the outset the TiO₂ have been grown on lithium niobate but the analysis has not been completed to establish the epitaxial relationship between the film and the substrate. Work is continuing on the deposition parameters to further improve the optical quality of the films.

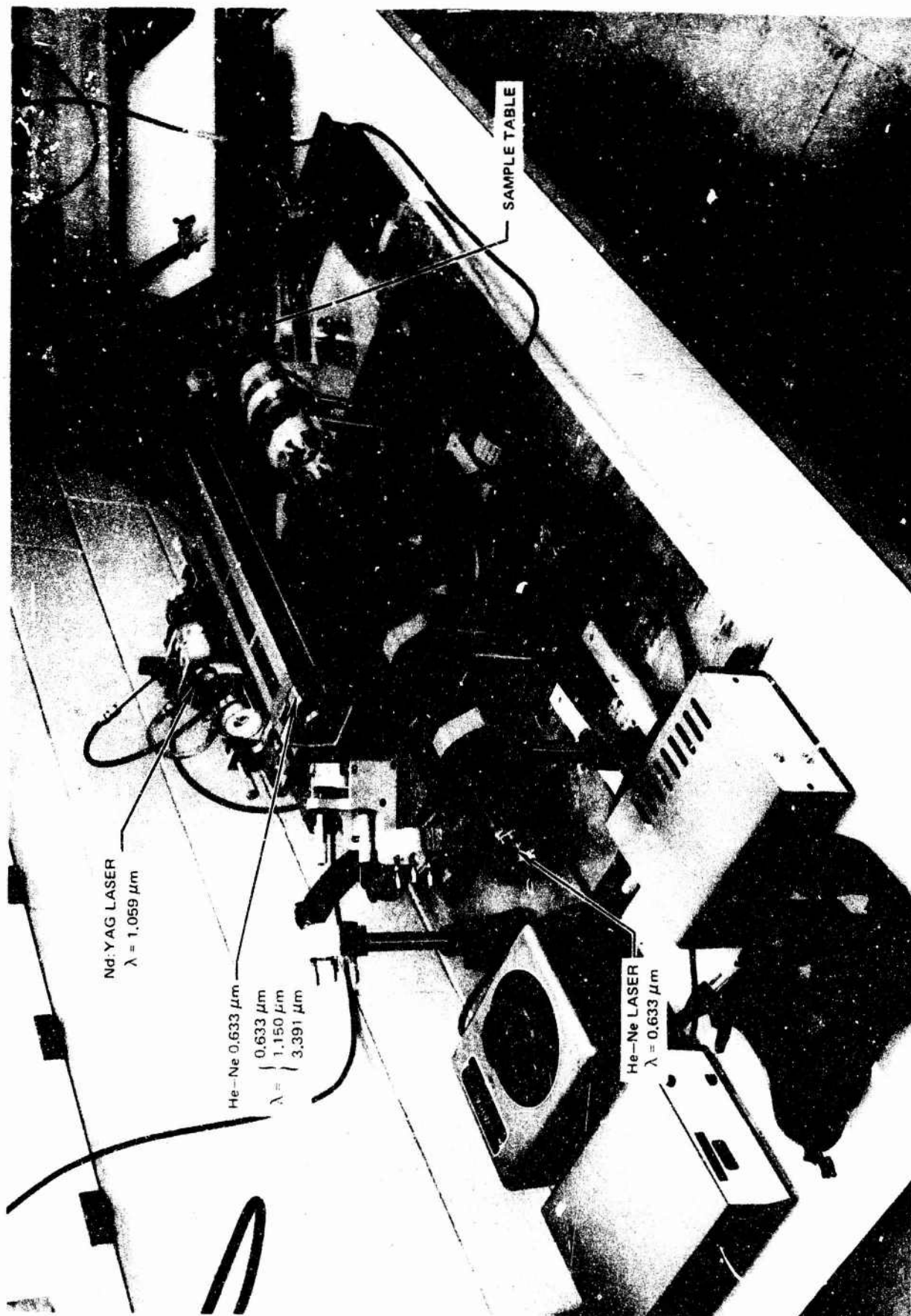
Gallium Nitride

The fixtures required for the reactive sputtering of gallium nitride were fabricated and assembled. Studies for epitaxial deposition of gallium nitride on sapphire and spinel have been initiated.

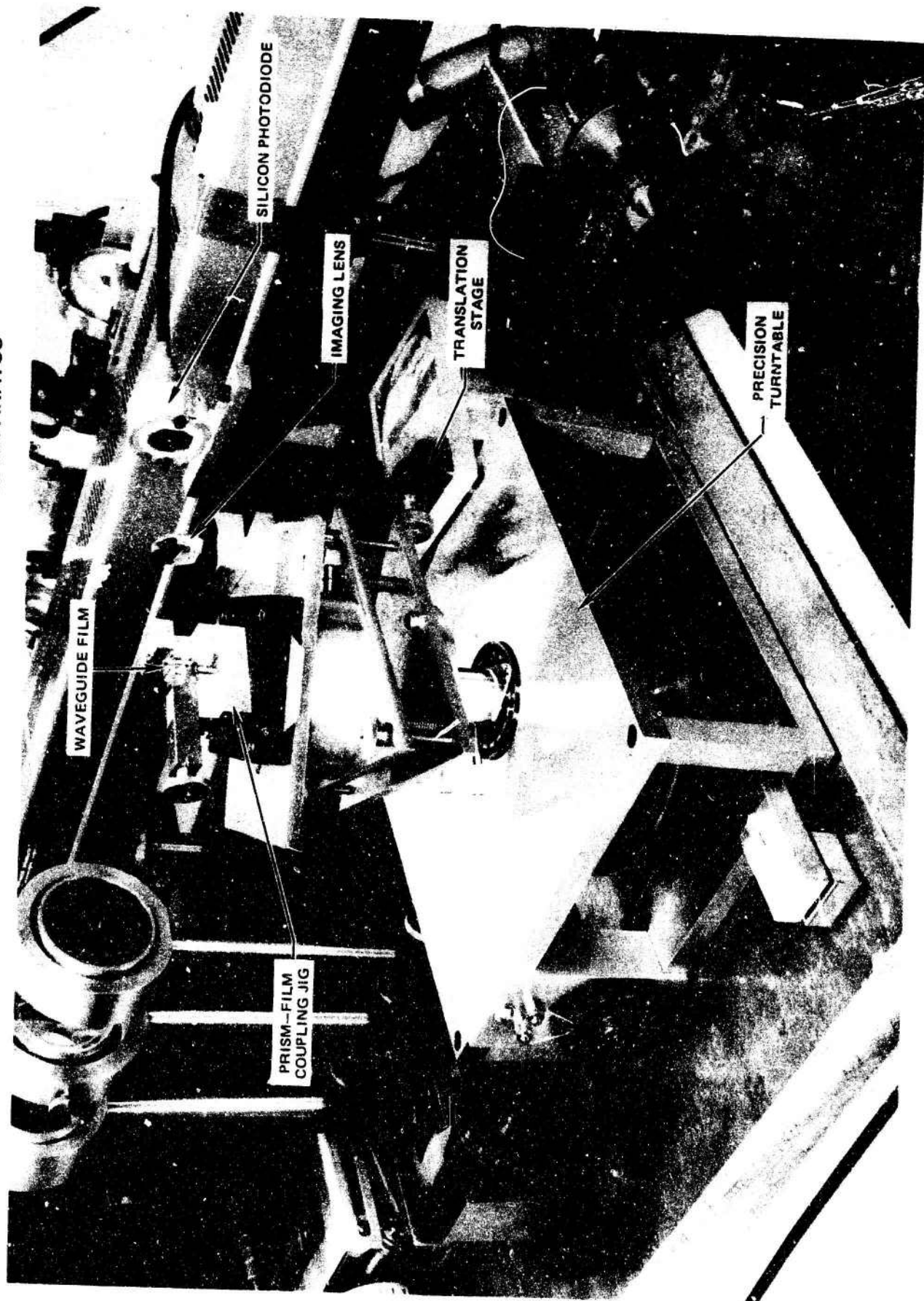
2.5 Future Work

Efforts will continue on the refinement of the deposition parameters to further improve the optical quality of the ZnO, AlN and TiO₂ films. In addition to optical evaluation, structures of the films will be examined using x-ray and reflection electron diffraction techniques. The films will be examined for gross structural defects by sectioning and examination by electron microscopy. In addition to the (0001) and (1 $\bar{1}$ 02) orientations of sapphire growth of ZnO, AlN and GaN on (11 $\bar{2}$ 0) and (10 $\bar{1}$ 4) orientations will be explored to determine if better optical quality films can be grown. Optical properties of films grown on (110) and (111) spinel substrates will be evaluated. Growth of TiO₂ on YZ cut LiNbO₃ will continue to be pursued. Device structures employing either acoustooptic or electrooptic interaction using the above materials will be fabricated to further evaluate the quality of the material grown.

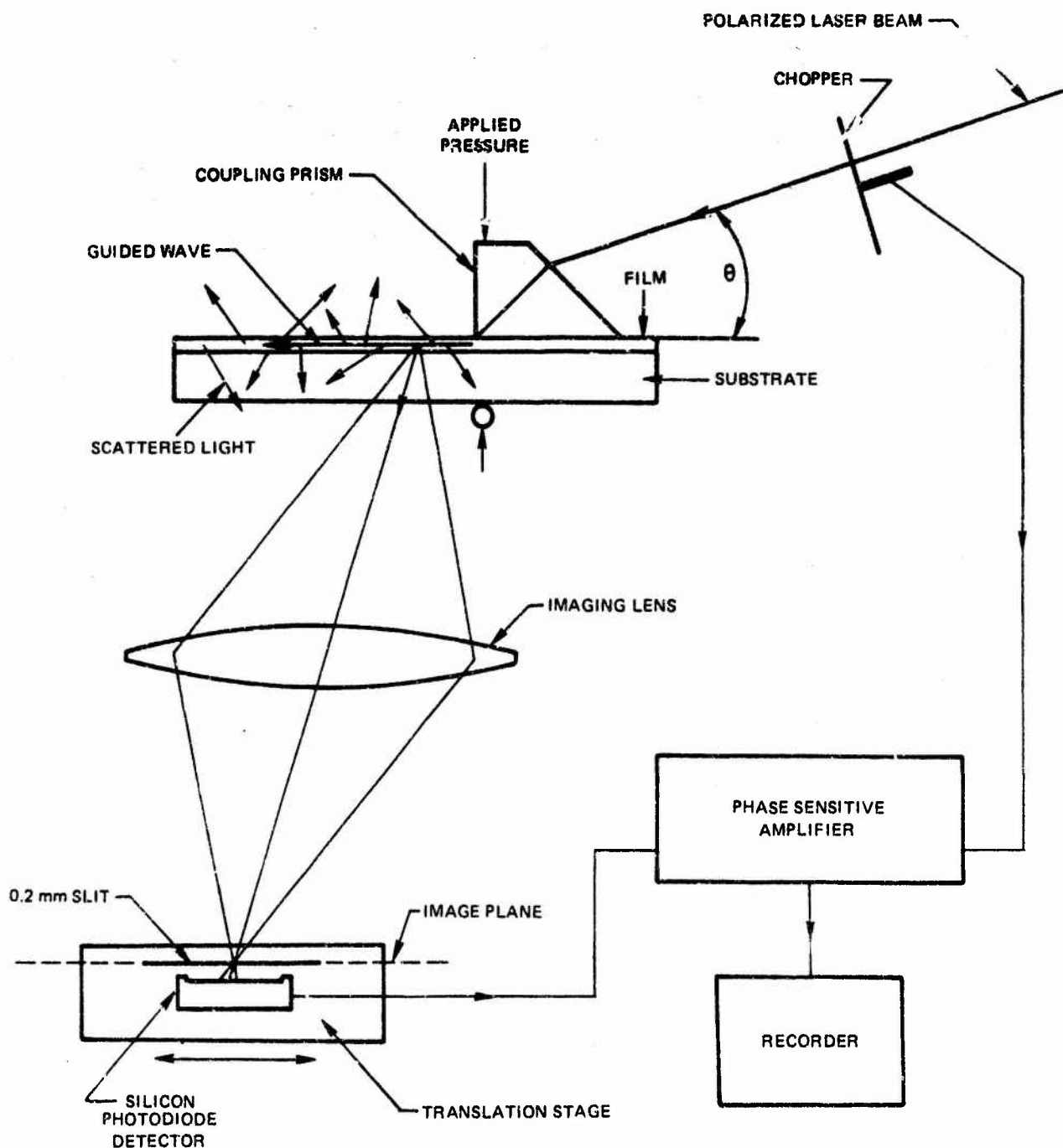
APPARATUS FOR STUDYING WAVEGUIDING IN THIN FILMS



SAMPLE TABLE & ATTENUATION MEASURING APPARATUS



EXPERIMENTAL SETUP FOR OPTICAL ATTENUATION MEASUREMENTS



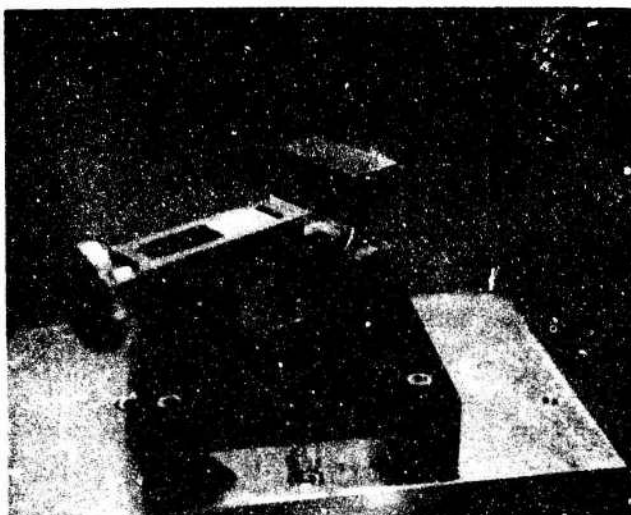
Ta₂O₅ FILM ON 7059 GLASS WAVEGUIDING



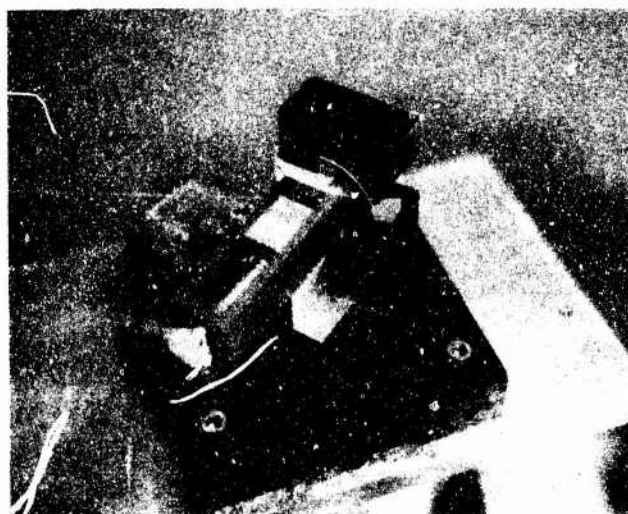
Ta_2O_5 FILM ON $0.1\ \mu$ FINISH SAPPHIRE SUBSTRATE



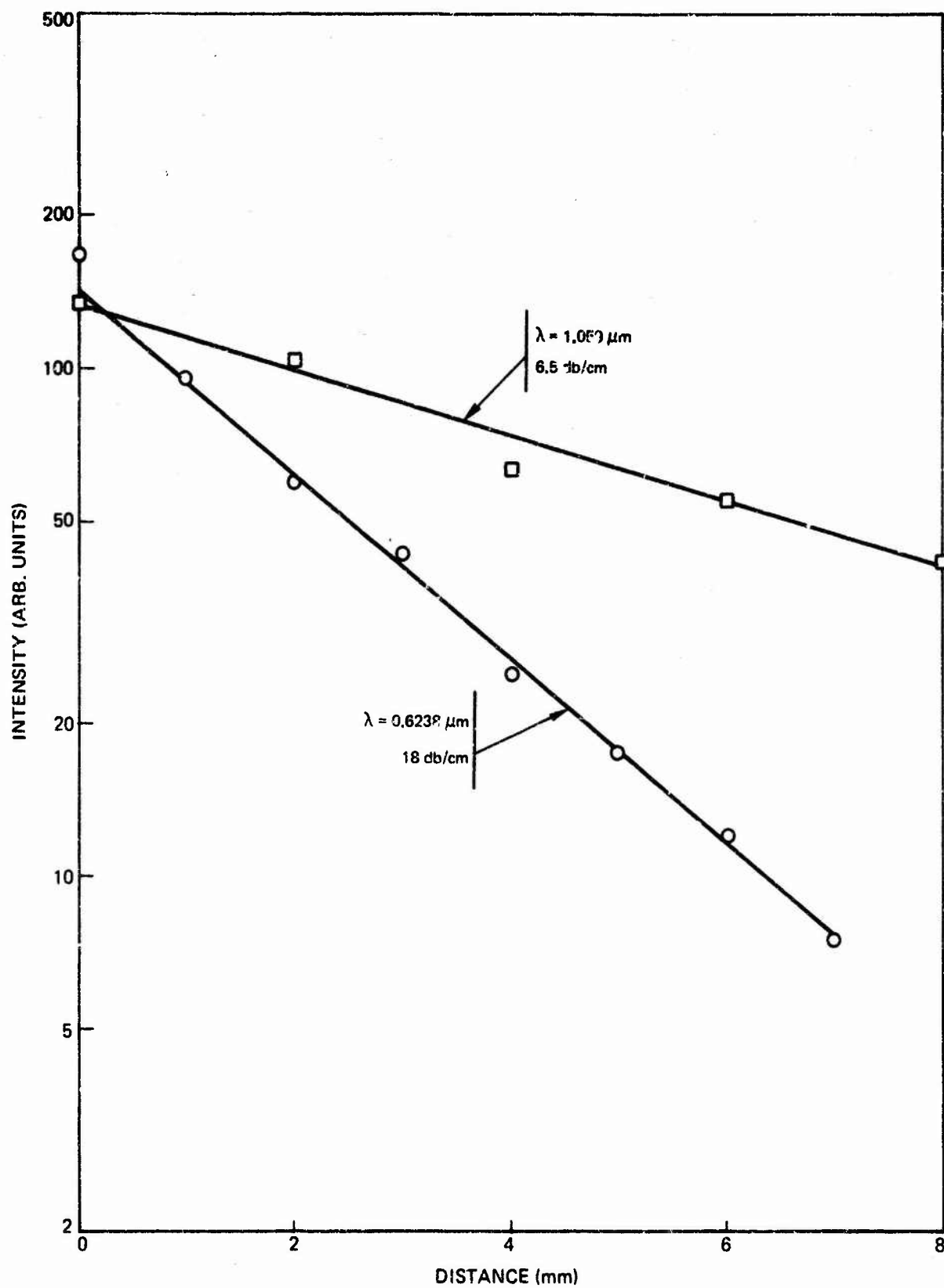
Ta_2O_5 FILM ON MELLER SAPPHIRE SUBSTRATE



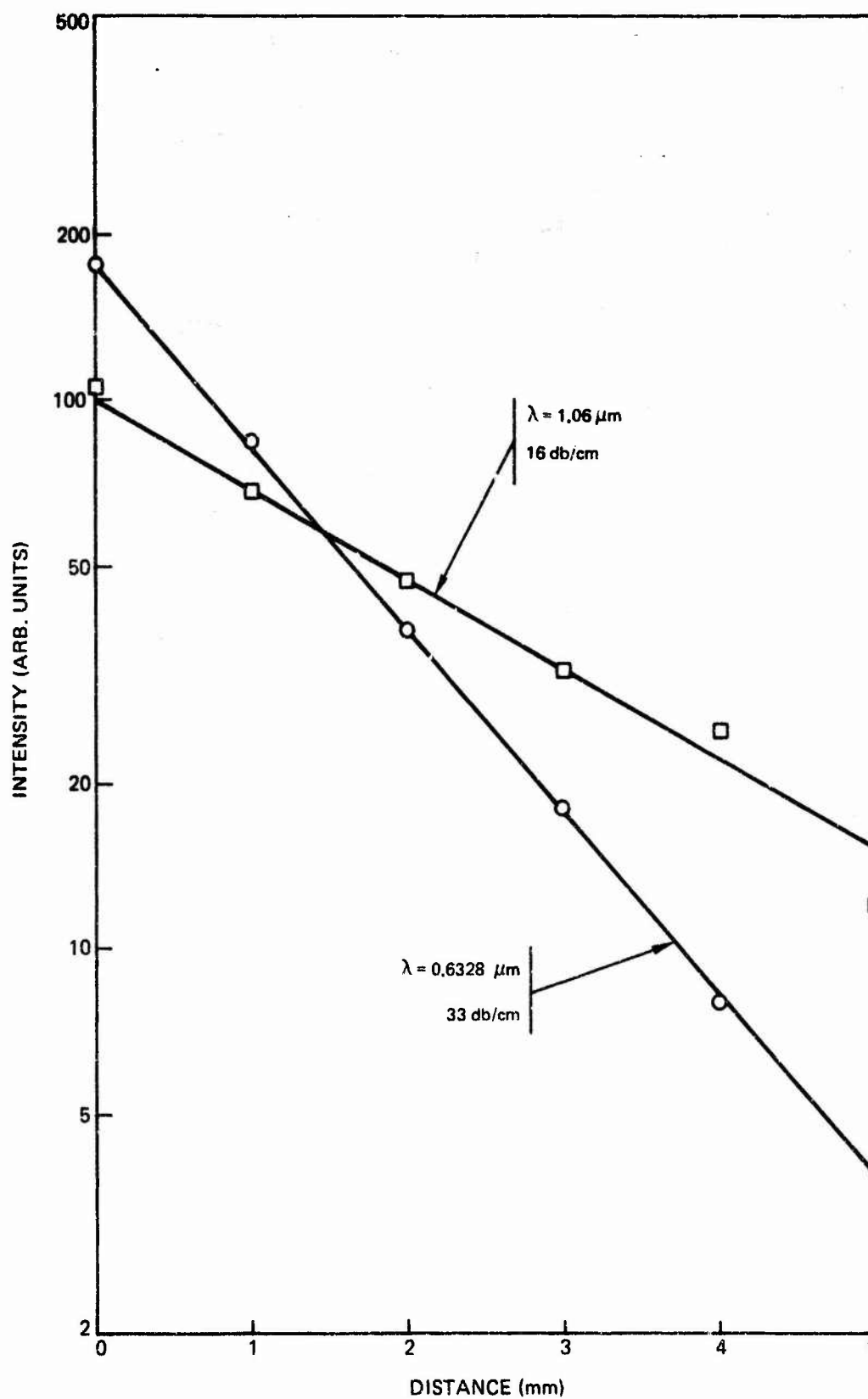
SINGLE CRYSTAL ZnO WAVEGUIDING



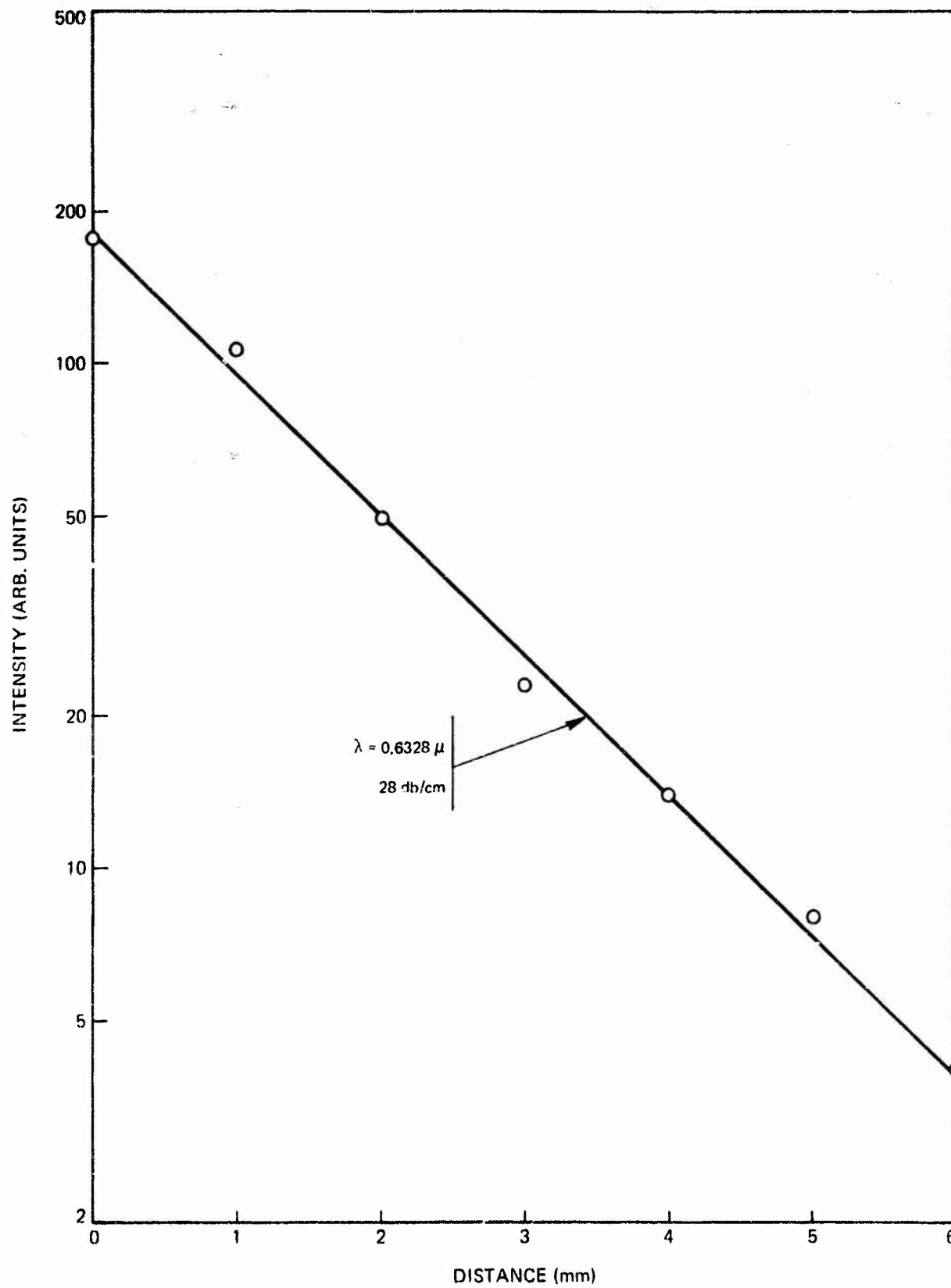
SAMPLE NO. ZnO-37
ZnO ON Al_2O_3 (1102)



SAMPLE NO. 119
AlN ON Al₂O₃ (0001)



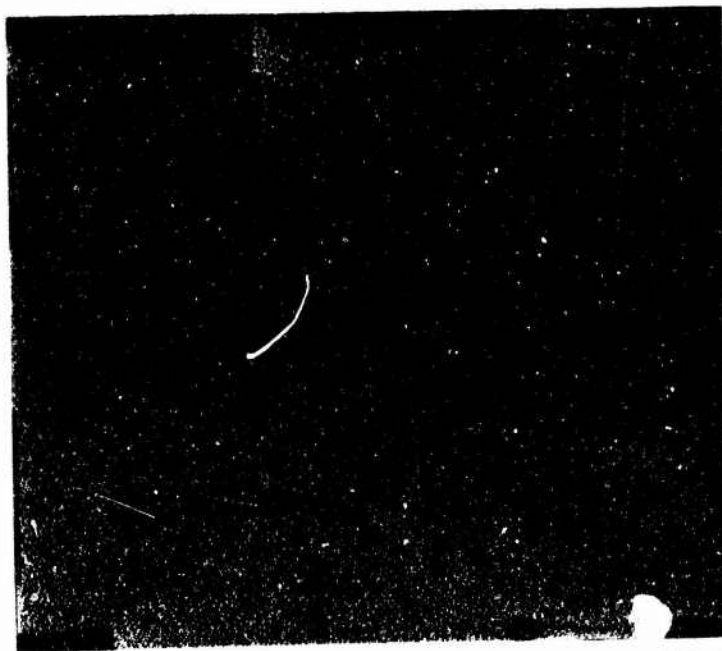
SAMPLE NO. 36

 TiO_2 ON LiNbO_3 

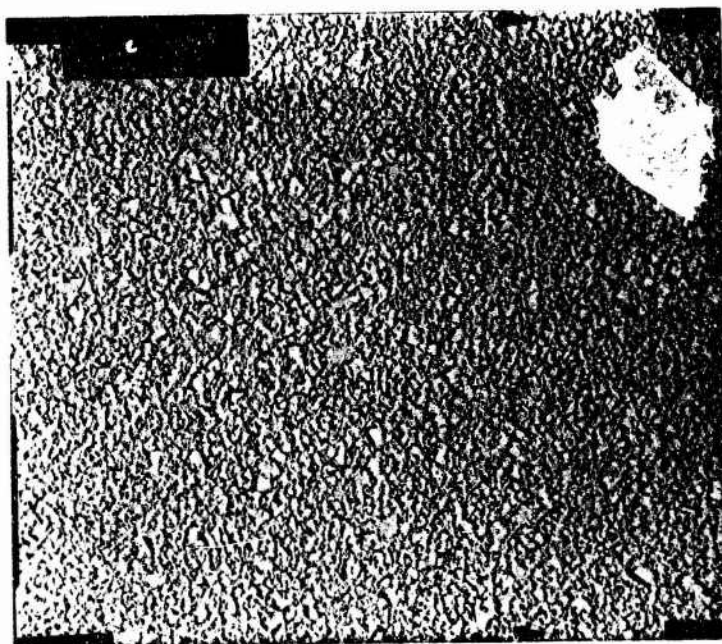
2-17

ELECTRON MICROGRAPH OF TiO_2 ON (0001) Al_2O_3

NO AXIAL FIELD RF POWER 150 W



4800X



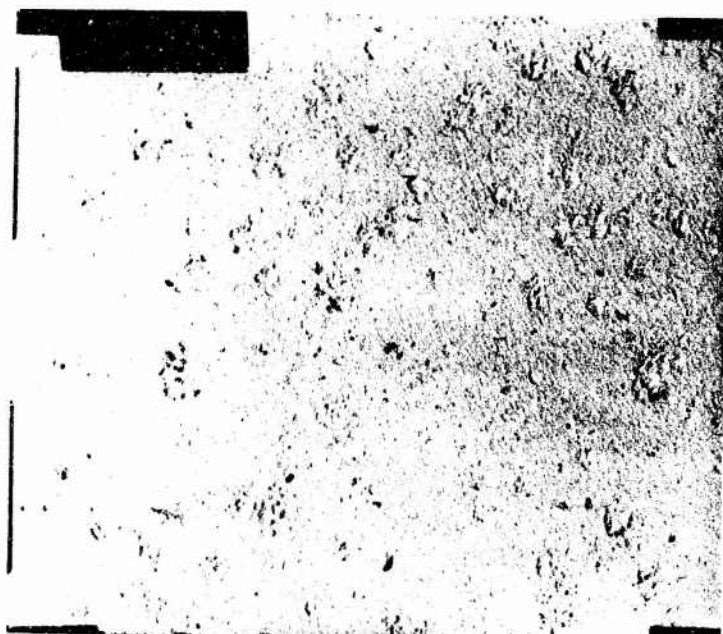
10,000X

ELECTRON MICROGRAPH TiO_2 ON (1102) Al_2O_3

NO AXIAL FIELD RF POWER 150 W



4800X



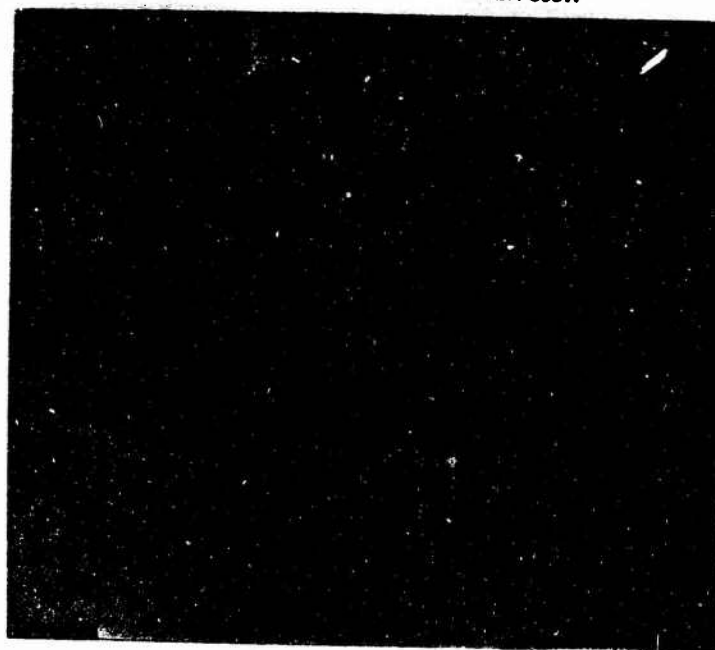
10,000X

2-20

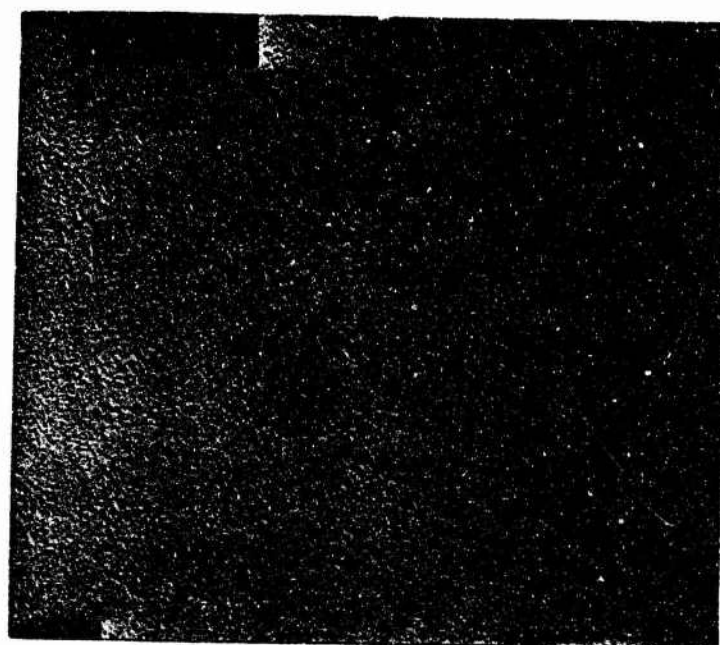
ELECTRON MICROGRAPH OF TiO_2 ON (0001) Al_2O_3

NO AXIAL FIELD

RF POWER 300W



4800X



10,000X

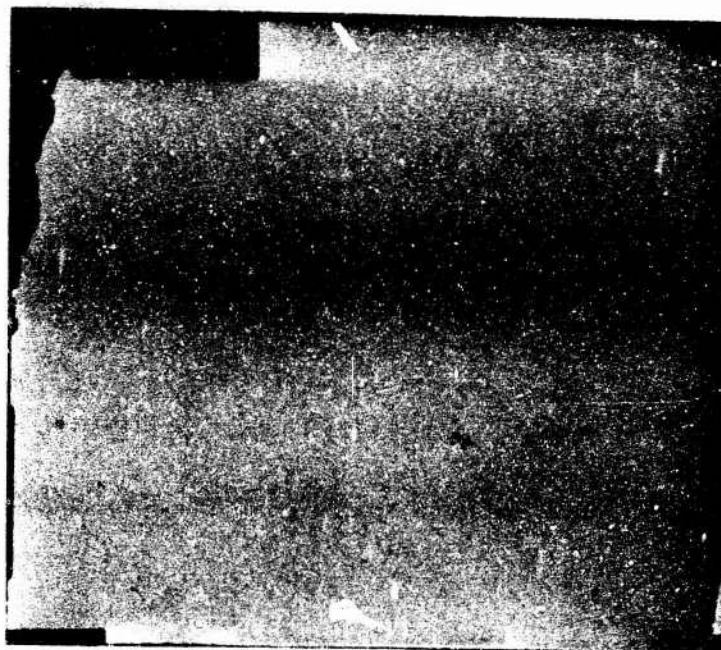
2-21

Reproduced from
best available copy.

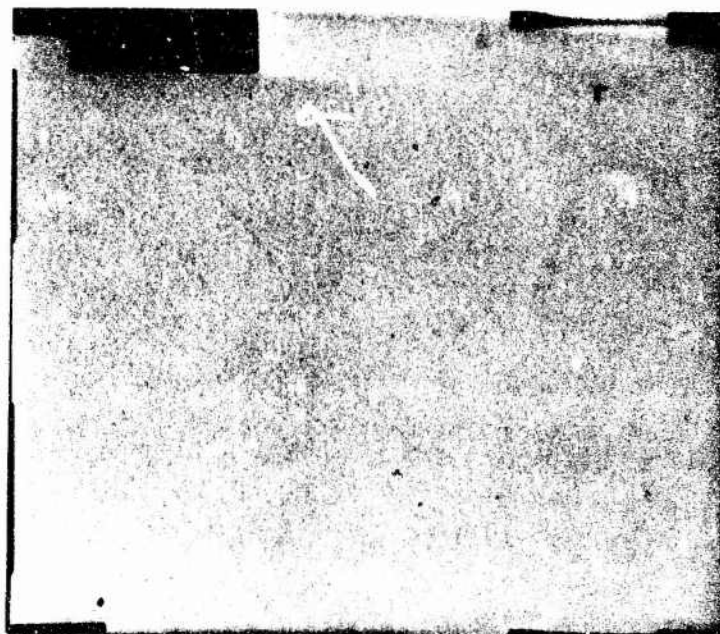


ELECTRON MICROGRAPH OF TiO_2 ON (0001) Al_2O_3

AXIAL FIELD RF POWER 300 W



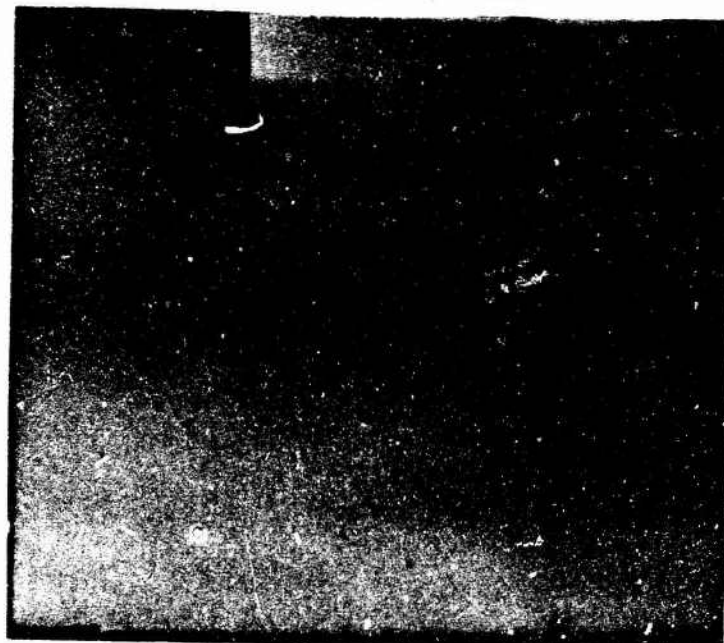
4800X



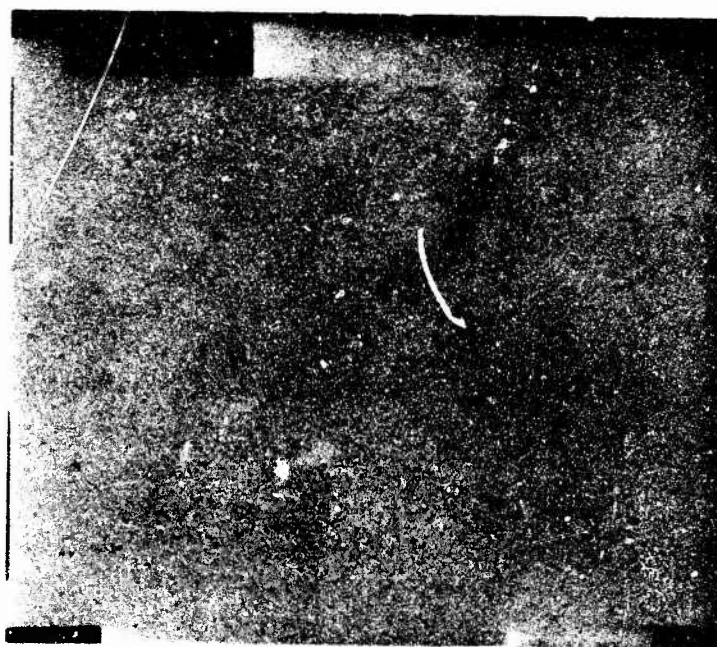
10,000X

ELECTRON MICROGRAPH OF TiO_2 ON $(1\bar{1}02) \text{Al}_2\text{O}_3$

AXIAL FIELD RF POWER 300 W



4800X



10,000X

Table 2-I

Sample ZnO-37

ZnO on Al_2O_3 ($1\bar{1}02$)

	<u>m</u>	<u>β/k Values</u>		
TE modes $N_F = 2.002$	0	1.991	1.991	< .001
	1	1.959	1.959	< .001
	2	1.904	1.904	< .001
	3	1.827	1.828	.001
TM modes $N_F = 1.991$	0	1.979	1.979	< .001
	1	1.945	1.944	.001
	2	1.888	1.885	.003
	3	1.810	1.805	.005

$$W = 1.372 \pm .010 \text{ } \mu\text{m}$$

3.0 GROWTH OF EPITAXIAL GALLIUM ARSENIDE FILMS*

This section of the report discusses the continuing effort to produce gallium arsenide epitaxial films of a quality suitable for integrated optics. During this report period more sensitive analytical techniques have been employed to determine both the impurity levels and stoichiometry of the sputtered GaAs films. The electrical properties of the epitaxial films are discussed in the light of their growth parameters. Preliminary experiments to determine the waveguide properties of the sputtered films are also reported. Further insight into how the sputtering parameters affect the quality of the films is being gained by an investigation of the epitaxial growth of InSb. These results are presented.

3.1 Sputter-Ion Spectroscopy of a GaAs Film

In order to further identify the cause of the anomalously low carrier mobility in the sputtered GaAs films, sputter-ion mass spectrographic analysis was employed. Depending on the particular impurity under analysis, concentrations as low as 20 ppb can be detected. As mentioned in the last report, the cause of the low mobility in the GaAs films could be due to scattering by structural imperfections and/or a large concentration ($\sim \leq 10^{20} \text{ cm}^{-3}$) of impurities. Since the electron microprobe technique initially used for impurity analysis can detect high 10^{19} cm^{-3} concentrations, it obviously cannot be used to detect the presence of several impurities whose concentrations add up to $\sim 10^{20} \text{ cm}^{-3}$. Table 3-I shows the results of the sputter ion analysis of sample Ga-23. Impurity determinations were made at depths of 4.7 μm and 14 μm below the original film surface. If the concentrations of the non-III-V elements are added, their total concentrations at these depths are $0.7 \times 10^{18} \text{ cm}^{-3}$ and $1.1 \times 10^{18} \text{ cm}^{-3}$, respectively. The presence of impurities at these levels could not account for the low measured mobilities. Since the spectral line of the Ga^{69} positive ion partially interfaces with the appearance of the copper line, the sensitivity of the analysis is limited to 2 ppm ($\sim 10^{17} \text{ cm}^{-3}$) for this impurity. Copper contamination has been a concern since copper gasketing is employed in the sputtering chamber. The rather large concentration of indium in the films cannot be traced to any component in the vacuum chamber. Spectrographic examination of the gallium target did reveal the presence of 24 ppm of indium. A separate analysis of the original gallium material showed less than 10 ppm indium; therefore, its presence must be due to an accidental contamination. Since indium and aluminum are group III elements, these will enter the lattice substitutionally and be electrically inactive. The possibility of strong alloy scattering from such a low concentration of these elements is highly unlikely.

The spectrum in Fig. 3.1 also reveals interesting facts about the nature of the argon-sputtered GaAs species. It is found that GaAs primarily dissociates on

*Analysis performed by F. G. Satkiewicz of GCA Corporation, Boston, Massachusetts.

sputtering to give As^+ , As_2^+ , As^{+2} , Ga^+ , Ga_2^+ , and Ga^{2+} . In addition, a much lower concentration of associated species like GaAs^+ exist in the plasma. Since the Ga target in the GaAs sputtering system is exposed to arsenic at elevated temperatures, a film of GaAs is formed on the Ga surface. Under normal sputtering conditions it is this film that supplies the Ga species. It is expected that the distribution of the various species when sputtering with As is similar to that found in the case of sputter-ion spectroscopy.

3.2 Electron Microprobe Determination of GaAs Stoichiometry

Since it appears that impurity scattering is not a reasonable explanation for the low observed carrier mobilities, a method to determine the presence of structural defects is required. Nonstoichiometry is a clear indication of structural defects. The electron microprobe can determine the composition of major constituents of a thin film to about 0.3%. This would be equivalent to a defect density $\sim 6 \times 10^{18} \text{ cm}^{-3}$.

For accurate analysis using the microprobe a standard is measured along with the unknown film. The standards used for this application are Bridgman, Cr-doped, semi-insulating, single crystal GaAs. A convenient way to prepare the standard-film pair on one substrate is to partially mask the substrate during GaAs film deposition. The standard and film can then be measured in alternate fashion. To improve the accuracy of the determination, the sample and standard are alternately measured ten times for each element. Two films along with separate standards were evaluated, and the consistency between standards was also corroborated by comparing one standard with respect to the other. The standards were assumed to be stoichiometric GaAs.

Table 3-II summarizes the results for these samples. The films were prepared using different growth conditions to determine whether changes in stoichiometry would result. Changes were made in substrate temperature, growth rate, and sputtering gas (see Table 3-III). Sample Ga-27, prepared at low temperature clearly indicates a deficiency in Ga and an excess in arsenic. The higher temperature sample is stoichiometric to within the accuracy of the technique. The importance of these measurements is that high concentrations of structural defects do exist in the sputtered GaAs films, and their density is sensitive to process parameters. It is most probable that structural defects below the detection limits do exist even in the higher temperature sample; these defects could be responsible for the low Hall mobility. Clearly then, this technique, although useful for demonstrating nonstoichiometry is not practical for optimizing the deposition process parameters as one approaches stoichiometry. From Table 3-II it can also be seen that the Ga deficiency is equal to the As excess. This would imply that Ga-vacancy-As-interstitial pairs are present.

3.3 Effect of Deposition Parameters on Sputtered GaAs

The deposition parameters that are readily controlled are: substrate temperature, deposition rate, sputtering gas and pressure, bias sputtering and choice of substrate material and its orientation. The nature of the deposited film is in part controlled by the substrate temperature in that amorphous, polycrystalline or single crystal films can be formed. In addition, since it was shown by sputter-ion mass spectrometry in Section 3.1 that the major sputtered species are Ga and As, a chemical recombination to form GaAs must occur on the substrate. Therefore, the substrate temperature influences the kinetics of this reaction. Depending on the deposition rate at a given temperature amorphous, polycrystalline or single crystal films can be formed. A high rate tends to produce the more disordered forms; however, under certain circumstances (e.g., in the case of a volatile constituent) a low rate might enhance vacancy formation. Also, impurities incorporated from the gas phase will be lowered by a high growth rate. The pressure of the sputtering gas affects the energy of the sputtered species via collisions with the ambient gas. Given any level of contamination in the sputtering gas an increase in pressure will result in a larger concentration of impurities in the deposited film. In the case of GaAs the concentration ratio of arriving species can be controlled by varying the As pressure in the system. This is necessary in order to accommodate the large difference in the sticking coefficient of the two elements. Sputtering at As pressures below that at which a plasma can be maintained can be accomplished by adding an inert gas. Choice of inert sputtering gas controls the deposition rate since sputtering is a momentum transfer process, and therefore, the rate goes as the square root of the molecular weight. Bias sputtering can affect film properties by removing weakly bonded impurities or host atoms in metastable positions (similar to annealing). At higher bias-sputtering energies, however, radiation damage can be introduced into the film.

In order to characterize the effect of variations in the above deposition parameters, RED, resistivity and Hall effect measurements were employed. Combined resistivity and Hall effect measurements lead to a value for the carrier mobility which is commonly used as an integrity factor for single crystal GaAs. The Hall mobility provides a measure of the ionized impurity content and is affected by the presence of structural defects on a microscale. Carrier concentrations derived from Hall measurements permit the calculation of the free carrier depression of the optical index and extent of free carrier absorption.

Since the number of process parameter combinations is so large, it was necessary to limit the investigation to extreme and mean values. Table 3-III is a compilation of the deposition parameters and electrical results made to date on GaAs films. RED measurements indicate that all of the films deposited on GaAs substrates were single crystal. The films grown on sapphire, however, were polycrystalline. A good RED pattern of a GaAs film grown on GaAs was shown in Fig. 20 of the last report. Films produced during this report period have predominantly high resistivities

and low Hall mobilities, and the obtaining of accurate electrical data continues to be a problem for films grown on GaAs. To ascertain a more accurate Hall mobility for GaAs, films were grown on sapphire. Even though these latter films are polycrystalline, their measured mobility is too low ($\mu < \text{cm}^2 \text{V}^{-1} \text{sec}^{-1}$) to be accounted for on the basis of grain boundary scattering and is, therefore, typical of the sputtered films. All the Hall measurements indicated a net n-type conductivity. The interesting effect of the substrate on obtaining accurate Hall data is exemplified by comparing films obtained from growth run 27. Although both films had almost identical resistivities, their calculated carrier mobilities differ by almost two orders of magnitude or more. The other values of mobility recorded in the table for the epitaxial films are also too high. Accurate resistivity values greater than $2 \times 10^4 \text{ ohm-cm}$ were not obtained due to shunting of current into the substrate.

Limitations on the accuracy of the above electrical data mask most trends with variation in the process parameters. Unless a fortuitous choice in the process parameters is made, optimization of these parameters for GaAs is impossible using electrical characterization techniques. Analysis for nonstoichiometry in these films (see Section 3.2) indicates that a film grown at a high substrate temperature is closer to stoichiometry than one at low temperature. This is also the direction towards higher resistivity where the electrical measurements become meaningless. In Section 3.5 preliminary results on a III-V semiconductor (InSb) with the same lattice structure as GaAs is presented. InSb is known to evaporate to give high carrier mobility and low resistivity films. It is hoped that by varying the process parameters for growth of InSb, information will be gained from electrical data which can be extrapolated to the GaAs system.

Some trends in the data of Table 3-III are discernable.

- (1) Higher substrate temperatures yield higher resistivities and higher growth rates for the same incident flux.
- (2) Bias sputtering using 22V to 79V did not lower the resistivity compared to one (Ga 22) grown without bias.
- (3) Changing the Ga/As ratio by a factor of 50 at temperatures near 560°C did not yield measurable changes in the resistivity.
- (4) Using argon as the sputtering gas decreases the sputtering rate (as expected).
- (5) Variations in the specific sputtering rate ($\text{\AA}/\text{min-w}$) also indicate that a chemical reaction occurs on the substrate. The increased reaction rate more than compensates for any decrease in the sticking coefficient of As.

From the above results, including the microprobe analysis for stoichiometry, it appears that growths at higher temperatures are preferred. It is felt that experience with InSb system will suggest the direction towards optimization of the GaAs system.

3.4 Optical Considerations and Results

An attempt was made to fabricate and evaluate a thin film optical waveguide utilizing a sputtered high resistivity ($\rho > 2 \times 10^4 \Omega\text{-cm}$) thin film of GaAs on an n^+ -GaAs substrate. Substrate preparation prior to growth included: slicing wafers from a (100) oriented Si-doped boule, lapping flat, and chemi-mechanically polishing on a rotating jig using sodium hypochlorite to $\sim 1.5 \mu\text{inch}$ rms finish. The substrates were cleaned with organic solvents, and any oxides were removed with an HCl etch, followed by deionized water and propanol rinses. All solvents used in the cleaning process were "electronic grade". Prior to deposition both the target and substrate were sputter cleaned (see run #41 in Table 3-III for the film deposition parameters).

An important design consideration for optical waveguides is the determination of the film thickness that will propagate at least a zero order mode. Since this thickness is a function of the difference in the index of refraction between the substrate and the film, as shown in Fig. 3.2, it is important that the Δn be determined. This curve was calculated for $1.06 \mu\text{m}$ radiation since that wavelength is in the range where a GaAs-based integrated optics technology would operate and is convenient for attenuation measurements using a Nd:YAG laser. The index difference between the GaAs substrate and an insulating GaAs film due to free carrier effects can be calculated from

$$\Delta n = - \frac{\frac{e^2}{2m^*} \epsilon_0 \omega^2}{n_i^2 - \frac{N_s e^2}{m^* \epsilon_0 \omega^2}} \Delta N$$

where n , e , m^* , ω , and N are the index of refraction, electronic charge, effective mass, operating frequency, and electron density, respectively. The calculated difference in index for GaAs at $1.06 \mu\text{m}$ for an N_s (substrate) of $2.8 \times 10^{18} \text{ cm}^{-3}$ is 5.6×10^{-3} . Another calculation based on reflectivity data of the sputtered film on this n^+ substrate between 3 and $10 \mu\text{m}$ and extrapolated to $1.06 \mu\text{m}$ gives a value of 3.5×10^{-3} for the index difference. This data was obtained by measuring the change in the reflectivity at the interference extrema and dividing by the value of the mean reflectivity at this wavelength. This is a direct measure of the index difference and does not require measurement of the absolute value of the indices to four significant places. This lower value of the index difference compared to that calculated from free carrier depression may be due to nonstoichiometry which will result in a decrease in the dipole concentration. The convergence of the $1.06 \mu\text{m}$ laser beam (0.2°) provides a low limit on Δn due to the inability to separate film modes from substrate modes. This corresponds to a Δn lower limit of 0.001 for

detection of waveguiding using this laser. As shown in Fig. 3.2, a GaAs film thickness greater than $\sim 1.8 \mu\text{m}$ is required to support a zero order mode. In order to insure wave propagation, the thickest film available, namely $2.5 \mu\text{m}$, on n^+ GaAs was initially chosen.

Another important design consideration is attenuation of the guided wave caused by losses in the n^+ substrate due to free carrier absorption. This attenuation has been calculated to be 81 dB/cm and 39 dB/cm for an index difference of 0.0035 and 0.0056, respectively, for the case of a zero-order TE mode at $1.06 \mu\text{m}$ wavelength passing through a $2.5 \mu\text{m}$ waveguide. Although this attenuation is high due to the film thickness and would probably mask other attenuating mechanisms, an attempt was made to observe guiding since its detection was possible.

The common approaches to coupling light into thin film waveguides are via prisms, gratings and focusing the light onto a cleaved edge of the device. At $1.06 \mu\text{m}$ the availability of transparent materials with an index greater than GaAs is very limited. Intrinsic GaAs, however, is a possible prism candidate. Boron phosphide does have the required optical properties but is not readily available as an optical component. In addition, the chances of GaAs cracking under stress applied through prism coupling is high. Coupling via a grating is the most effective technique for waveguide coupling but submicron grating spacings are required at $1.06 \mu\text{m}$. Gratings of this periodicity require laser generated interferograms of photoresist be fabricated on the waveguide. An apparatus to generate these gratings is under construction. In the meantime experiments on direct coupling via a focused laser beam have been attempted. This experiment was performed by focusing a Nd:YAG laser beam ($1.06 \mu\text{m}$) onto the cleaved edge of the film and substrate with a 25 cm focal length lens. Provision was made for rotating the plane of the film with respect to the beam. A "snooperscope" was used to observe any $1.06 \mu\text{m}$ radiation that might be scattered from a guided mode in the sample. The optical bench used in this experiment is shown in Fig. 2.1. Substrate modes were easily observed in these experiments. These were characterized by a broad angle of acceptance at low incident angles. No sharp film modes could be detected. Reasons for the inability to observe film modes are the high substrate attenuation and the inefficient manner of coupling light into the film. Since the focused beam is $50 \mu\text{m}$ in diameter and the film thickness is $2.5 \mu\text{m}$, less than 10% of the light is directly incident on the edge of the film. As a result the intensity of any trapped wave would be low compared to the intensity of any substrate mode. Subsequent films for waveguiding will be grown thicker since substrate attenuation and surface scattering decrease with increasing thickness for a given mode.

3.5 Sputtered Indium Antimonide Films

Thin films of InSb with high carrier mobility were first produced by Gunther (Ref. 8) by evaporating In and Sb by the method of three temperatures. Since this

material can readily be deposited in thin film form having near bulk-like electrical properties and having the highest reported Hall mobility of all the III-V compounds, the effect of changes in sputtering parameters on the electrical properties can be readily ascertained. The structure of GaAs and InSb is the same, and therefore, they should have many of the same structural problems on being sputtered. Electrical measurements are possible on the InSb films, and this data should permit the optimization of the sputtering parameters. Any trends observed in the sputtering of InSb will then be extrapolated to GaAs. Obviously, this approach is valid only if defects exist in sufficient quantity to affect the electrical properties, and their formation is similar to that in GaAs.

An InSb target was fabricated by melting a boule of InSb in a carbon mold. The carbon mold was inductively heated in vacuum. The InSb target was attached to the electrode in the high temperature sputtering chamber. An excess of antimony was obtained in two ways: first, by heating Sb in a crucible as was the case with As and second, by placing Sb directly onto the InSb target. The sticking coefficient of the sublimed Sb on the chamber walls is high and the vapor does not go through the elbow and reach the ionization gauge. Sputtering the excess Sb appears to be a more controlled technique for this process.

Single crystal films of InSb were deposited on both InSb and GaAs substrates. This was verified by RED as shown in Figs. 3.3, 3.4, 3.5, and 3.6. Polycrystalline films of InSb were grown on AlN, sapphire and spinel. Deposition conditions for these films are given in Table 3-IV. All the deposited InSb films exhibit low resistivity and high mobility compared to the GaAs films, and their electrical properties are easily measured when grown on semi-insulating GaAs substrates. As a result correlations of the electrical data with sputtering parameters can now be made. The electrical properties of the InSb films are shown in Table 3-V. All films exhibit n-type conductivity at room and liquid nitrogen temperature and show a slight decrease in carrier concentration at low temperature. The observed carrier concentrations are much too low to limit the mobilities via impurity scattering to the measured values. If impurity scattering were dominant, a concentration of $\sim 2 \times 10^{19} \text{ cm}^{-3}$ would be required to give these values. Compensation by impurities to levels of $\sim 10^{17} \text{ cm}^{-3}$, although possible, is highly unlikely to occur in such a reproducible fashion in all the InSb samples. Therefore, the combination of the low mobility and low carrier concentration leads to the conclusion that some type of systematic structural defect exists in sputtered InSb.

Substrate temperature, the method of providing excess Sb, and to a lesser extent, deposition rate, were the growth parameters initially varied. Argon pressure was maintained essentially constant during these runs. The most notable effect on the value of the Hall mobility is the method by which the excess Sb was introduced. This is an important parameter since the sputtering chamber cannot be heated high enough to permit Sb to reach the shielded ionization gauge, and therefore, the partial pressure of Sb at the substrate is unknown. Judging from deposition of Sb on the chamber surfaces and the loss of Sb from the crucible, a finite

excess of Sb must exist for runs 1 through 6. This must also be the case for runs 8 and 9 in which the excess Sb was sputtered from the target. On the average slightly higher Hall mobilities are observed when Sb is introduced through sublimation. The effect is probably due to the amount of excess antimony rather than to the technique of its induction. Comparing these results to run 7, in which no excess Sb was present, it is clear from the low Hall mobility of this sample that an excess of Sb is an important condition. With regard to substrate temperature the high Hall mobility and low carrier concentration of sample 5 suggest that high temperature growths should be employed as a part of the optimization procedures. Deposition rates varied from 55 to 621 Å/min for samples 1 and 4, respectively, and no large differences in the electrical properties were observed. In general the specific sputtering rate (Å/min-w) should be constant provided the sticking coefficient is independent of temperature. The specific sputtering rate as seen in Table 3-IV is not constant and with the exception of runs 2 and 4, higher deposition rates in the excess antimony runs are associated with higher temperatures. A chemical reaction on the substrate surface is therefore indicated, and the variables, temperature and the concentration of the reacting species, control the value of this quantity. The agreement in specific rate between runs 8 and 9 where all the growth parameters were constant is good. Although the sputtering conditions were nominally the same between runs 2 and 6, the Sb pressure may have differed.

3.6 Conclusions

Sputtered GaAs films show inordinately low carrier Hall mobilities due to lattice defects. Independent evidence for this conclusion arises from the measured nonstoichiometry and insufficient impurity concentrations in these films. The slightly lower than expected index of refraction for these films may also be due to the presence of lattice defects.

When the sputtering parameters are correlated with the film characteristics, several trends appear to exist. Substrate temperature affects the film stoichiometry and determines the film growth rate for a given flux of sputtered GaAs. Higher substrate temperatures tend to result in higher growth rates and produce more-stoichiometric and higher resistivity films. It is concluded that elevated temperatures enhance the removal of arsenic from metastable sites or prevent arsenic from occupying these sites. Since the film growth rate is increased at higher substrate temperatures, the reaction rate of the gallium atoms with the growing surface must be enhanced. The observation that the gallium deficiency and arsenic excess are equal indicates that the two defects exist as pairs. The pair defect could consist of a gallium vacancy and arsenic interstitial. The energetics of the growth process will control which defect is initially formed. This defect would be present in a metastable state and be responsible for the formation of the other. The possibility of an arsenic atom occupying a gallium site and so account for the nonstoichiometry is energetically less likely.

Electrical results on epitaxially sputtered InSb lead to the tentative conclusion that defects are limiting the carrier Hall mobility as in sputtered GaAs. Since there is a preliminary indication that the film growth rate increases with substrate temperature, chemical recombination on the surface is occurring with InSb as well as GaAs. InSb sputtered onto a high temperature substrate gave the highest Hall mobility and lowest carrier concentration at room temperature. This direction towards higher growth temperatures agrees with the trend towards more stoichiometric films for GaAs grown at high temperatures. InSb sputtered without excess antimony yields a film with poor electrical characteristics.

Since the lack of efficient coupling techniques has prevented observable waveguiding no conclusions can be drawn at this time concerning the attenuation mechanism in sputtered GaAs films.

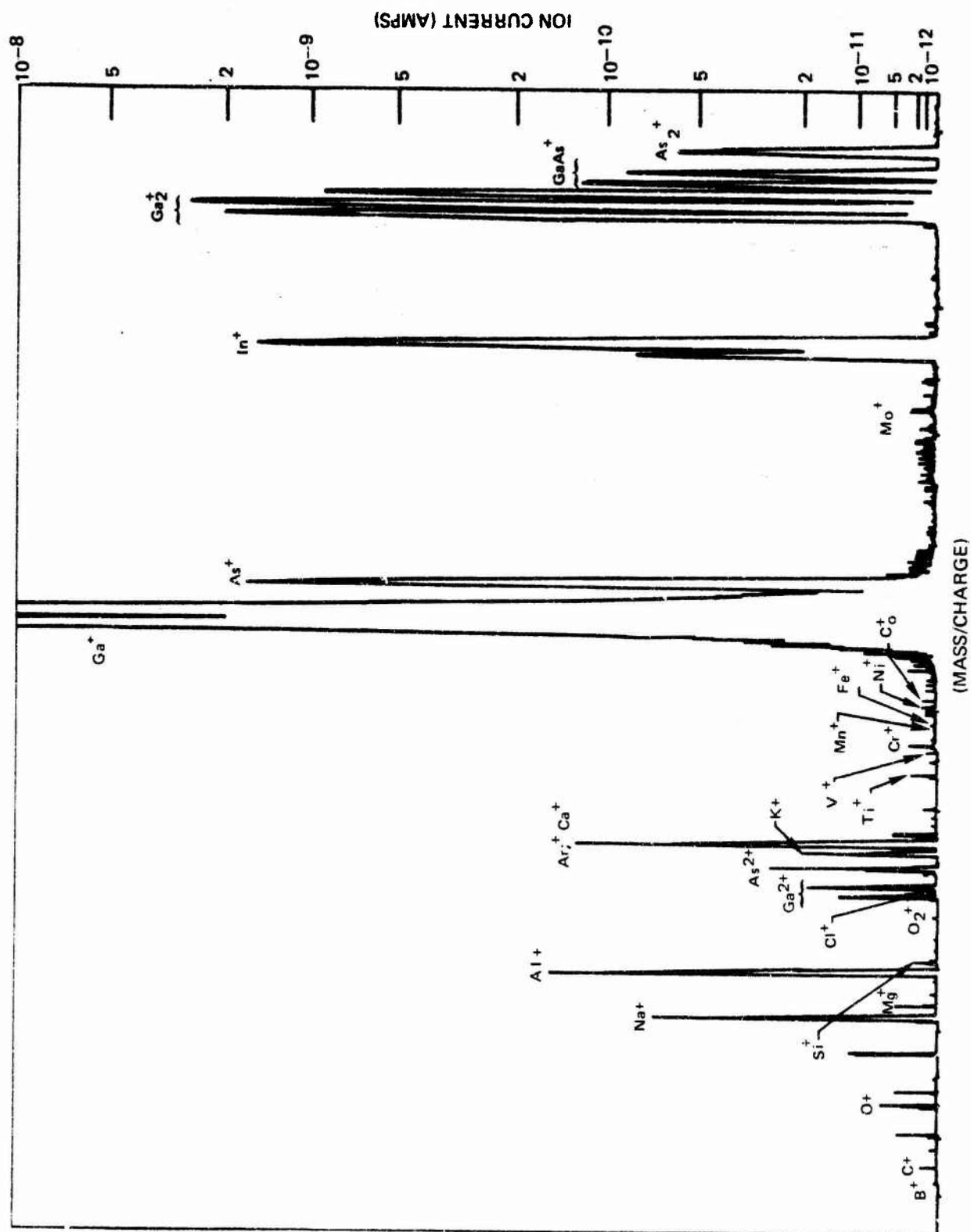
3.7 Future Work

Initial emphasis will be placed on improving the coupling coefficient into the sputtered GaAs films. This will be accomplished by the use of gratings, which will be fabricated by interferometrically exposing photoresist with a split laser beam. After waveguiding at $1.06 \mu\text{m}$ is observed, attenuation measurements will be made. Attenuation due to scattering can be separated from bulk absorption by attenuation measurements at other wavelengths. These experiments will be done if appropriate lasers become available.

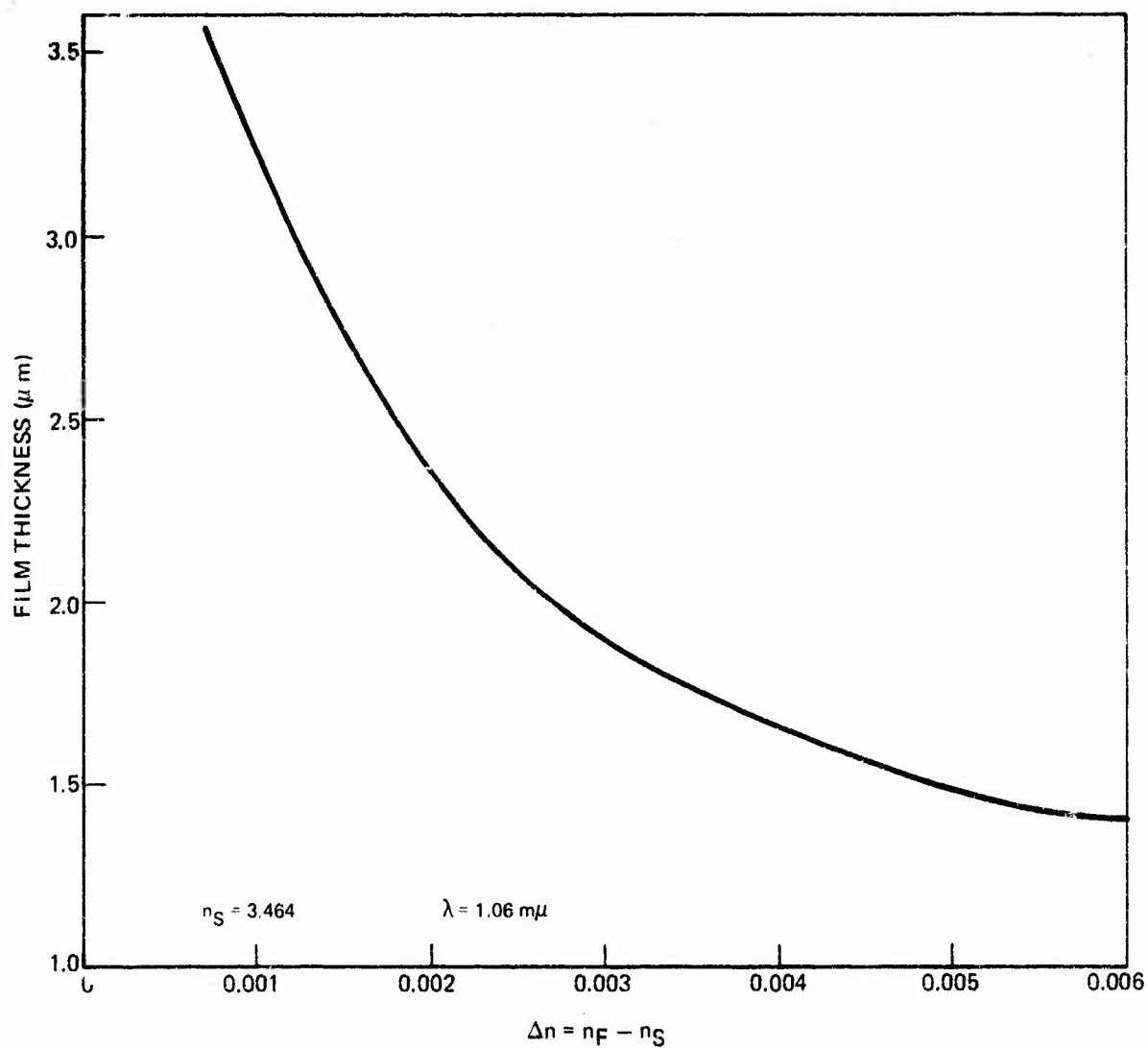
The growth of InSb films will continue in an effort to discover trends relating deposition parameters with electrical properties and stoichiometry. Electron microprobe analysis of both stoichiometry and impurities will be employed. If the vapor pressure of Sb is determined to be the limiting factor in controlling the carrier mobility, then InAs may have to be substituted. InAs has also been deposited in thin film form having high carrier mobility, and the As pressure in the sputtering chamber can be well controlled. The effect of As pressure on the properties of the resultant InAs films could then be evaluated and applied to GaAs.

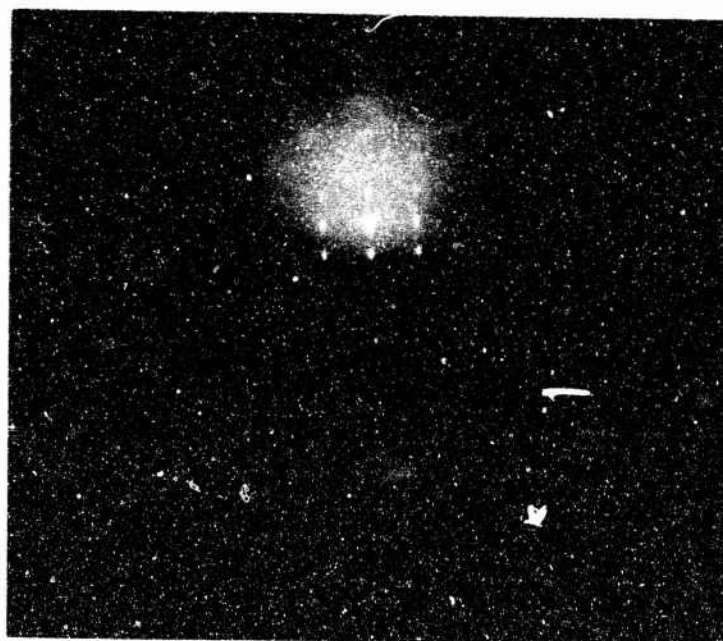
The results of the above investigations in III-V epitaxial growth will be extrapolated to the GaAs system. Subsequently, an attempt to grow $\text{Ga}_x\text{Al}_{1-x}\text{As}$ under similar conditions will be made so that additional waveguide structures can be fabricated.

SPUTTER-ION MASS SPECTRUM OF A GaAs FILM

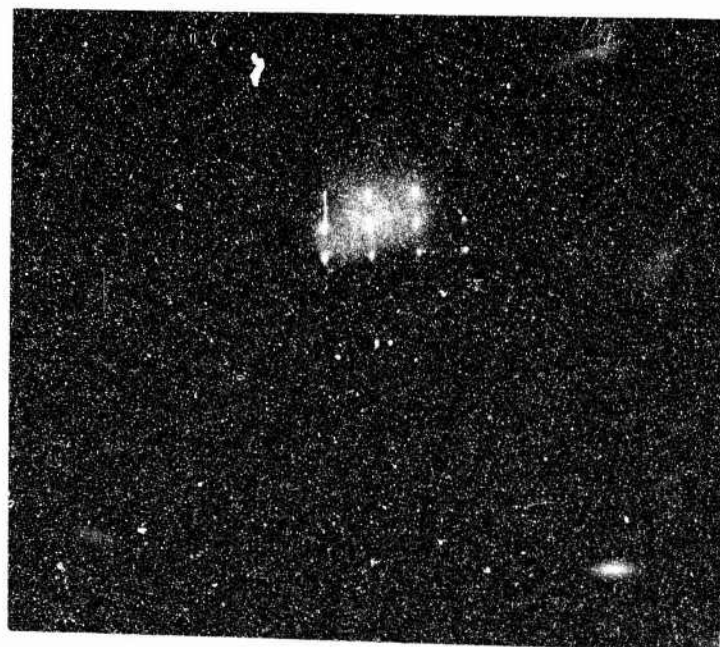


MINIMUM FILM THICKNESS REQUIRED TO SUPPORT $m = 0$ MODE VS. INDEX
DIFFERENCE BETWEEN FILM AND SUBSTRATE



REC OF (111) InSb—BEAM ALONG $[\bar{2}11]$ 

InSb SUBSTRATE PRIOR TO GROWTH



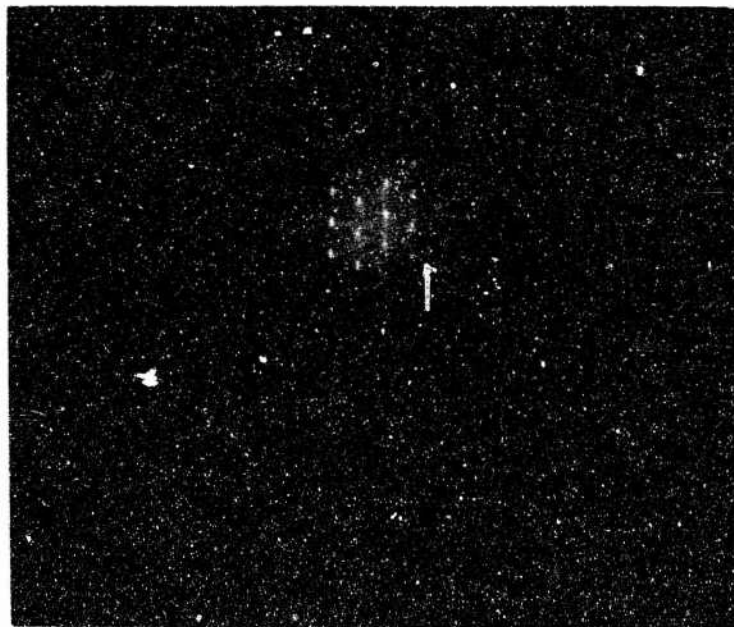
SPUTTERED InSb FILM ON InSb

Reproduced from
best available copy.

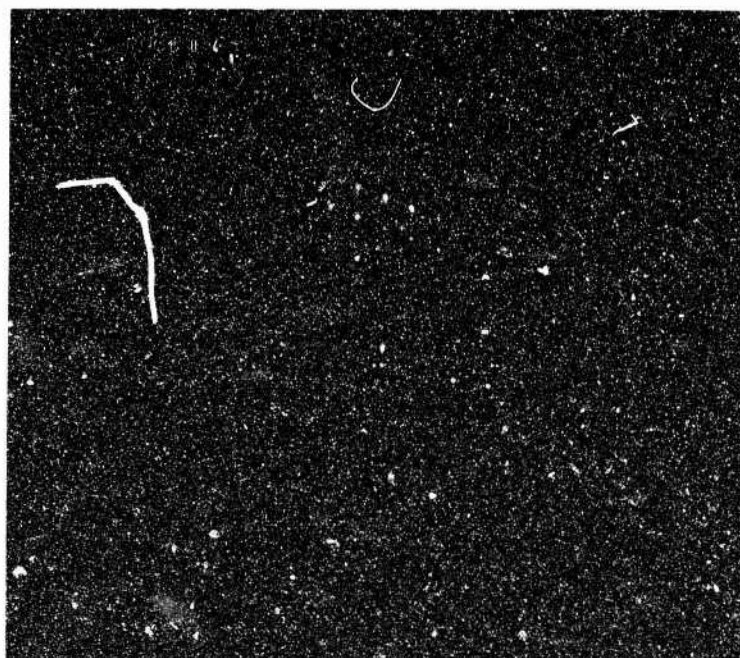


3-12

RED OF (111) InSb—BEAM ALONG $[1\bar{1}0]$



InSb SUBSTRATE PRIOR TO GROWTH

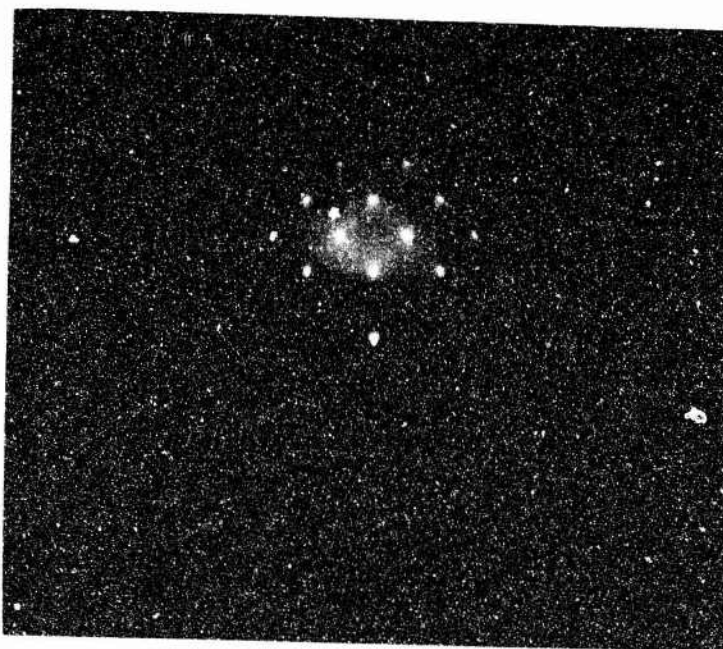


SPUTTERED InSb FILM ON InSb

RED OF InSb ON (100) GaAs—BEAM ALONG [100]



GaAs SUBSTRATE PRIOR TO GROWTH

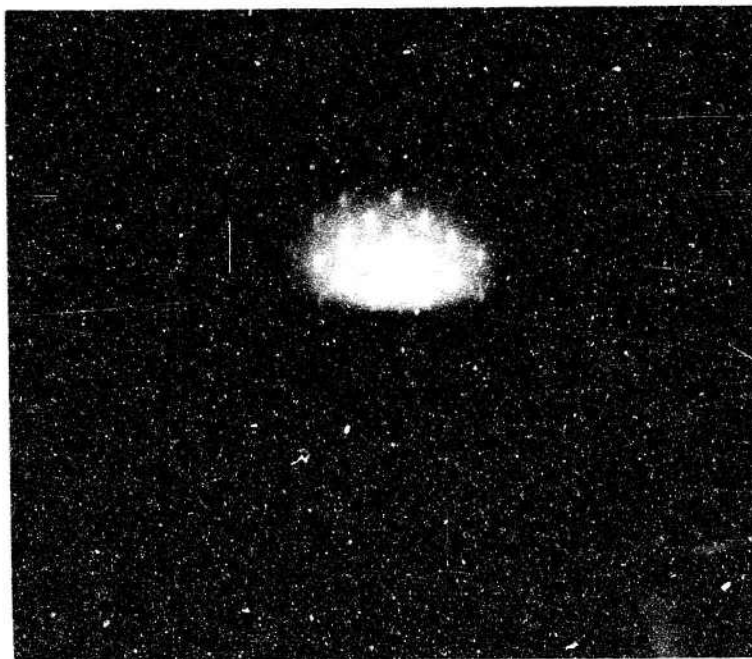


SPUTTERED InSb FILM ON GaAs

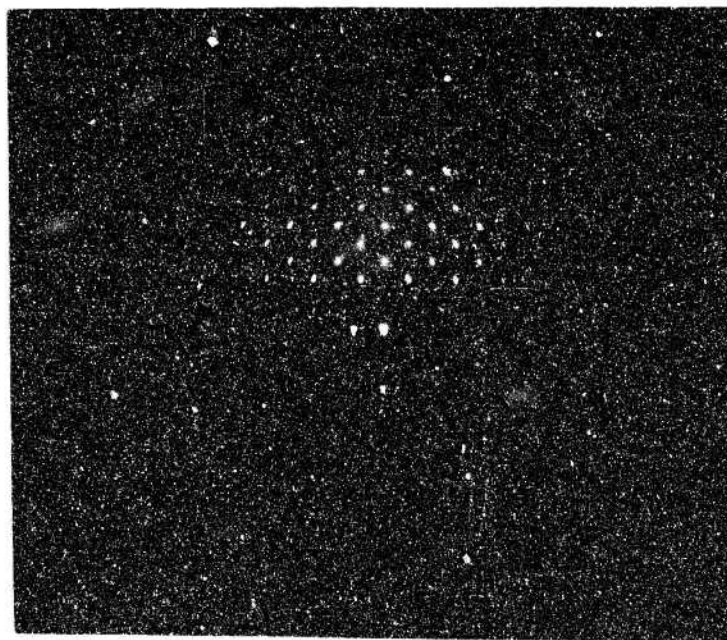
Reproduced from
best available copy.



RED OF InSb ON (100) GaAs—BEAM ALONG [110]



GaAs SUBSTRATE PRIOR TO GROWTH



SPUTTERED InSb FILM ON GaAs

3-15


Reproduced from
best available copy. 

Table 3-I

Mass Spectrographic Analysis of a Gallium Arsenide Film
(Sample Ga-23)

Species	ppm, atomic	
	<u>4.7 μm depth*</u>	<u>14 μm depth*</u>
B		~ 1
C	3	3
O	5	6
Na	0.4	1.4
Mg	~ 0.2	1.4
Al	8	17
Si	1	1.2
Cl		0.4
K	0.2	0.06
Ca		2.2
Ti	0.02	0.14
V	2.2	0.6
Cr	0.8	0.9
Mn	~ 2	1
Fe	~ 1	1.4
N:	N.D. **	~ 2
Co		~ 0.4
Cu	N.D. **	
Mo	~ 1	3.6
In	600	650

*Depth from film surface

**N.D. - not detected

3-16

Table 3-II

DETERMINATION OF STOICHIOMETRY BY ELECTRON MICROPROBE ANALYSIS**MEAN CHEMICAL COMPOSITIONS AND TWO SIGMA LIMITS BASED ON 10 ANALYSES****SAMPLE 41**

<u>ELEMENT</u>	<u>ATOMIC PERCENT</u>
Ga	49.92 ± 0.40
As	50.06 ± 0.40

SAMPLE 27

<u>ELEMENT</u>	<u>ATOMIC PERCENT</u>
Ga	48.52 ± 0.32
As	51.48 ± 0.32

STANDARD

<u>ELEMENT</u>	<u>ATOMIC PERCENT</u>
Ga	50.00 ± 0.53
As	50.00 ± 0.53

Table 3-III

Deposition Conditions and Electrical Properties of GaAs Films

Growth Run	Substrate Temp. (C°)	Deposition Rate Å/min (Å/min-watt)	Sputtering Pressure (mm)	ρ (ohm-cm)	Observed Mobility cm ² V ⁻¹ sec ⁻¹
(100) Cr-Doped GaAs Substrates					
17	375	280 (2.2)	20-25-As	9×10^3	< 10
20	375	1070 (4.3)	25-30-As	$> 2 \times 10^5$	< 20
21	375	130 (2.4)	25-As	---	--
22A	450	190 (3.4)	21-As	$> 2 \times 10^5$	--
23	375	1460 (3.0)	25-As	---	--
25	330	50 (1.0)	30-40-As	157	7.5
27	330	85 (1.3)	~ 40-As	54	1.3
32	555	230 (3.0)	< ~ 15-As	$> 3 \times 10^4$	--
35	555	270 (1.9)	0.3-As, 60-Ar	$> 3 \times 10^4$	--
39 [22V]*	495	45	~ 10-As, 15-20-Ar	$> 3 \times 10^4$	--
41 [50V]*	490	330	~ 5-As, 2-Ar	$> 2 \times 10^4$	--
43 [67V]*	460	160	~ 5-As, ~ 10-Ar	$> 2 \times 10^4$	--
44 [61V]*	490	75	~ 3-As, ~ 10-Ar	$> 2 \times 10^4$	--
45 [79V]*	490	90	~ 10-As, ~ 7-Ar	$> 2 \times 10^4$	--
46	490	50 (1.6)	< 0.1-As, 7-Ar	---	--
*Bias sputtering runs, applied rms voltage in brackets					
Sapphire Substrates					
20 (0001)	375	1070	25-30-As	---	--
21 (0001)	375	130	25-As	8.8×10^3	< 1
21 (1102)	375	130	25-As	---	--
27 (0001)	330	95 (1.5)	~ 40-As	48	< 0.2

Table 3-IV

Deposition Parameters for InSb Films

Run #	Substrate Temp. (°C)	Deposition Rate $\text{\AA}/\text{min}$ ($\text{\AA}/\text{min-w}$)	Sputtering Pressure (μm of Ar)
1-C-(111) Spinel	415	621 (4.2)	14
1-C-(1102) Sapphire	415	590 (4.0)	14
2-C	375	435 (5.0)	30
4-C	435	55 (2.5)	23
5-C-AlN	465	220 (4.5)	16
6-C	375	320 (3.7)	28
7-O	375	450 (5.4)	25
8-S	375	340 (3.9)	23
9-S	375	320 (3.7)	29

C - Sb supplied by heated crucible, sputter InSb

O - No extra Sb source, sputter InSb

S - Sb pieces placed on InSb target to provide excess Sb

Table 3-V
Electrical Properties of InSb Films

Run #	Room Temperature Electrical Properties			77°K Electrical Properties			
	$\rho(\text{ohm-cm})$	$n(e^-/\text{cc} \times 10^{17})$	$\mu(\text{cm}^2 \text{V}^{-1} \text{sec}^{-1})$	ρ	n	μ	
1-C-Al ₂ O ₃	6.8×10^{-3}	2.1	4340	1.2×10^{-2}	----	----	
2-C	2.4×10^{-3}	4.2	6340	3.0×10^{-3}	3.4	6130	
4-C	6.5×10^{-3}	2.8	3980	8.5×10^{-3}	2.4	3120	
5-C-AlN	1.9×10^{-2}	0.40	8240	3.7×10^{-1}	0.32	530	
6-C	7.1×10^{-3}	1.7	5200	1.6×10^{-2}	0.79	4910	
7-0	1.8×10^{-2}	1.6	2175	2.8×10^{-2}	0.34	6440	
8-S	3.1×10^{-3}	4.5	4420	3.5×10^{-3}	3.9	4580	
9-S	5.3×10^{-3}	4.1	2875	6.9×10^{-3}	3.0	2960	

4.0 GROWTH OF SPUTTERED LASER MATERIALS

A totally integrated optical technology must include elements that produce gain. Lasers meet these requirements, and for this application should be fabricated in thin-film form. One technique for achieving this goal is to optically pump a thin-film laser material with a light emitting diode (LED) such as GaAs or its mixed alloys. In particular GaAs-type LEDs can be used to pump the 8000Å to 9000Å absorption bands of the neodymium ion, which is properly spaced in a host lattice like yttrium aluminum garnet (YAG). The solubility of neodymium in the garnet lattice is one-to-two percent. This limits the gain per unit length of the laser and requires large geometries. To be compatible with integrated optics, materials exhibiting much higher gain are required. Laser action has recently been demonstrated in 35-micron-long platelets of neodymium ultraphosphate ($\text{NdP}_5\text{O}_{14}$) (Ref. 9). Dimensions of this magnitude are ideally suited for integrated optics applications. This material has also lased, but with increased threshold, in the amorphous state. This is an important fact since the heteroepitaxy of single crystal $\text{NdP}_5\text{O}_{14}$ via sputtering would probably require temperatures above 800°C. These high temperatures would not be compatible with a GaAs-based technology. Furthermore, due to the orthorhombic crystal structure of $\text{NdP}_5\text{O}_{14}$, epitaxial growth on the zinc-blend GaAs structure is unlikely. At elevated temperatures the sticking coefficient of Nd, P, and O will vary and give rise to stoichiometry problems. In light of the above, a low temperature deposition of an amorphous film of $\text{NdP}_5\text{O}_{14}$ would more likely yield a thin film laser.

Neodymium ultraphosphate was synthesized by heating neodymium oxide (99.9% pure) with excess orthophosphoric acid (electronic grade) to ~ 500°C in a Pd-Au crucible. During the heating schedule, which is performed under a dry oxygen flow, the orthophosphoric acid predominantly loses water to form higher phosphoric acids, and an insoluble crystalline phosphate, $\text{NdP}_5\text{O}_{14}$, is eventually precipitated.

Identification of $\text{NdP}_5\text{O}_{14}$ was accomplished through x-ray powder diffraction using copper K_α radiation and a Debye camera. This material is orthorhombic with cell constants, 12.95, 8.7, and 8.93, for the a, b and c axes, respectively, and is reported to belong to the space group P_{mna} (Ref. 10). Since no ASTM card is available for this compound, the observed diffraction lines were compared with those calculated from the unit-cell parameters taking into account space group extinctions. Using this information all the "d" spacings of the 38 observed lines between 2θ values of 19° and 82° could be assigned Miller indices. Table 4-I lists the overall good agreement between observed "d" spacings with "d" spacings calculated from possible (hkl) reflections for $\text{NdP}_5\text{O}_{14}$.

Several runs for producing $\text{NdP}_5\text{O}_{14}$ were carried out in order to obtain sufficient material for the fabrication of a four inch sputtering target. At present we are in the process of determining the parameters for hot pressing this material into a target.

A sputtering system is being specifically modified for the deposition of this type of material. Provision has been made for the sputtering of both hot pressed and powdered targets. Pressed targets are more suitable since small particles from a powdered target can become charged and embed themselves in the growing film. Powdered targets are convenient and more economical for studying the conditions for stoichiometric growth. Substrates can be both heated and cooled (100°K - 1000°K) as well as sputtered cleaned. Initial depositions will be made on 7059 glass substrates in an oxygen or argon-oxygen plasma at low substrate temperatures. Stoichiometry and impurity content will be determined by electron microprobe and spectrographic analysis, respectively. If sputtered $\text{NdP}_5\text{O}_{14}$ amorphous films can be grown, both absorption and gain measurements will be performed.

Table 4-I

Powder X-Ray Diffraction Data for $\text{NdP}_5\text{O}_{14}$

<u>Line</u>	<u>I/I₀</u> (eyeball)	<u>"d" (obs)</u>	<u>Possible</u> (hkl)	<u>"d" (cal)</u>
1	40	4.462	002	4.465
2	15	4.304	020	4.365
3	20	3.763	112	3.800
4	100	3.651	202	3.676
5	20	3.613	220	3.619
6	10	3.346	212	3.388
7	10	3.227	400	3.238
8	10	3.106	022	3.121
9	10	3.013	122	3.034
10	100	2.895	030	2.910
11	10	2.806	013	2.817
12	20	2.603	402	2.621
13	10	2.518	322	2.529
14	10	2.436	023	2.459
15	10	2.405	511	2.392
16	20	2.246	004	2.233
17	10	2.168	600	2.158
18	20	2.132	204	2.111
19	5	1.947	503	1.954
20	100	1.937	620	1.935
21	10	1.908	341	1.903
22	10	1.871	242	1.877
23	5	1.802	440	1.810
24	100	1.785	622	1.775
25	10	1.753	050	1.746
26	5	1.679	442	1.677
27	5	1.637	052	1.626
28	5	1.573	524	1.577
29	5	1.538	640	1.535
30	5	1.526	614	1.528
31	10	1.461	060	1.455
32	10	1.384	062	1.383
33	20	1.325	036	1.325
34	10	1.301	163	1.301
35	15	1.243	070	1.247
36	50	1.203	072	1.201
37	20	1.185	536	1.180
38	10	1.167	037	1.168

5.0 REFERENCES

1. P. K. Tien, Applied Optics, 10, 2395 (1971).
2. The authors are indebted to Dr. Fritz Zernike of Perkin-Elmer Research Laboratories for his assistance during the initial stages of the optical waveguiding study.
3. M. L. Dakss, L. Kuhn, P. F. Hendrich and B. A. Scott, Appl. Phys. Lett., 16, 523 (1970).
4. J. E. Goell and R. D. Standley, B.S.T.J., 48, 3445 (1969).
5. W. L. Bond, J. of Appl. Phys., 36, 1674 (1965).
6. J. M. Hammer, D. J. Channin, M. T. Duffy and J. P. Wittke, Appl. Phys. Lett., 21, 358 (1972).
7. M. J. Brady, M. Levanoni and A. Reisinger, Optics Comm., 7, 390 (1973).
8. K. G. Gunther, Z. Naturforsch, 13a, 1081 (1958); K. G. Gunther and H. Freller, Z. Naturforsch, 16a, 279 (1961).
9. H. P. Weber, T. C. Damen, H. G. Danielmeyer and B. C. Tofield, Appl. Phys. Lett., 22, 534 (1973).
10. H. G. Danielmeyer and H. P. Weber, Journal Quantum Electronics, QE-8, 805 (1972).